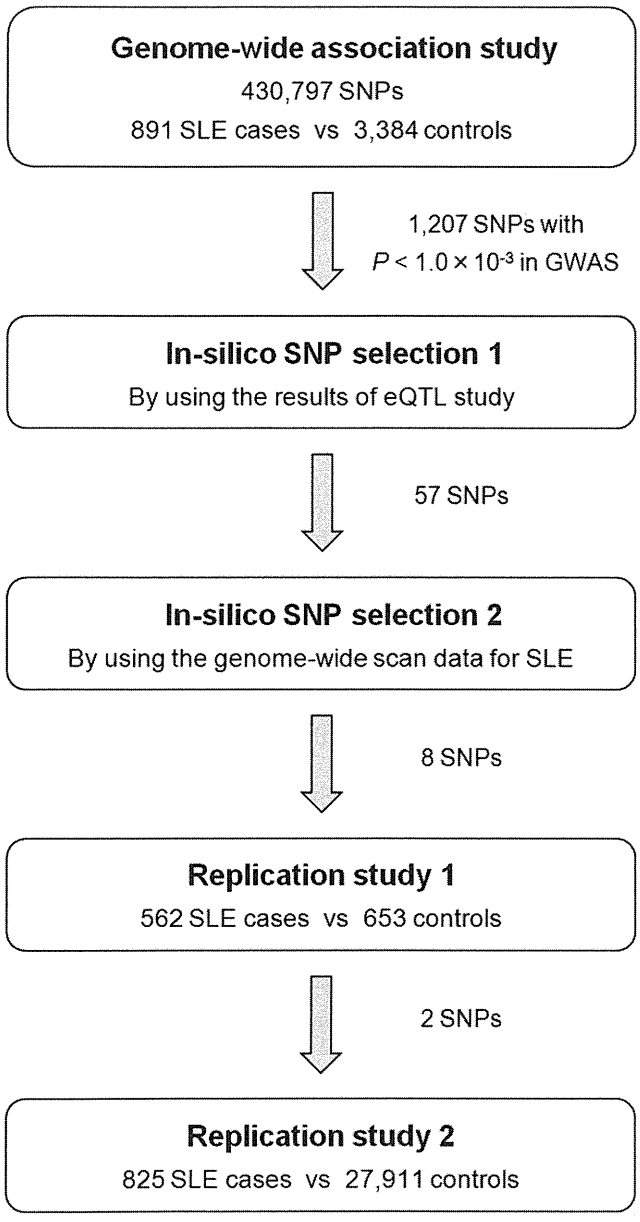

Figure 1. Design of the GWAS and multi-stage replication studies for SLE in Japanese subjects. A total of 2,278 SLE cases and 31,948 controls were enrolled. The clinical characteristics of the subjects are summarized in Table S1 and S2. Details of the genome-wide scan data for SLE referenced in the *in silico* SNP selection 2 are described elsewhere (Tahira T et al. Presented at the 59th Annual Meeting of the American Society of Human Genetics, October 21, 2009).
doi:10.1371/journal.pgen.1002455.g001

pooled analysis. As a result, 8 SNPs remained for further investigation (Table S4).

Replication studies and identification of *AFF1*

Then, we performed two-stage replication studies using independent SLE cohorts for Japanese subjects (cohort 1 with 562 SLE cases and 653 controls, and cohort 2 with 825 SLE cases and 27,911 controls). First, we evaluated the selected 8 SNPs in the replication study 1. In the replication study 2, 2 SNPs that satisfied $P<1.0\times10^{-6}$ in the combined study of GWAS and replication study 1 were further evaluated (Figure 1). Among the evaluated SNPs, we observed significant replications in the SNP located in the genomic region of the AF4/FMR2 family, member 1 gene (*AFF1*) at 4q21 (rs340630; $P=4.6\times10^{-5}$ and $P=0.0094$ in the two individual cohorts, respectively; Table 3, Table S5, and Figure 2B). The combined study for the GWAS ($P=1.5\times10^{-4}$) and the replication studies demonstrated significant associations of rs340630 that satisfied the genome-wide significance threshold ($P=8.3\times10^{-9}$, OR = 1.21, 95% CI 1.14–2.30).

Cis-eQTL effect of rs340630 on *AFF1* transcripts

Since the landmark SNP in the *AFF1* locus, rs340630, was prioritized through the eQTL study as an eQTL positive SNP (Table 3), we further validated its cis-eQTL effect using Epstein-Barr virus (EBV)-transfected B cell lines established from Japanese individuals (Pharma SNP Consortium (PSC) cells, $n=62$). The correlation between rs340630 genotypes and the expression levels of *AFF1* was significant in the PSC cells stimulated with phorbol myristate acetate (PMA) ($R^2=0.074$, $P=0.033$; Figure 3A). The expression levels increased with the number of SLE-risk (A) alleles. To further confirm this cis-regulatory effect, we performed allele-specific transcript quantification (ASTQ) of *AFF1*. The transcript levels of each allele were quantified by qPCR using an allele specific probe for a SNP in the 5′-untranslated region (rs340638), which was in absolute LD with rs340630 ($r^2=1.0$, $D'=1.0$). We examined PSC-cells ($n=17$) that were heterozygous for both rs340630 and rs340638. The mean ratio of each transcript (A over G allele; the A allele comprises a haplotype with the risk (A) allele of rs340630) were significantly increased to 1.07 compared to the ratio of the amount of DNA (1.00, $P=0.012$) (Figure 3B). These results suggest that rs340630, or SNP(s) in LD with it, are a regulatory variant predisposing SLE susceptibility through increased expression levels of *AFF1*.

Expression of *AFF1* in $CD4^+$ and $CD19^+$ peripheral blood lymphocytes

AFF1 is known to be involved in cytogenetic translocations of acute lymphoblastic leukemia (ALL) [31]. Its fusion protein with the mixed-lineage leukemia gene (*MLL*) is implicated in the regulation of transcription and the cell cycle of lymphocytes [31]. To investigate the expression pattern of *AFF1* in normal tissues, we evaluated the transcript levels of *AFF1* in a panel of various tissues. We observed prominent expression of *AFF1* in $CD4^+$ and $CD19^+$ peripheral blood lymphocytes, implying an important role for *AFF1* in helper-T-cells and B-cells (Figure 3C).

Discussion

Through a GWAS and multi-staged replication studies consisting of 2,278 SLE cases and 31,948 controls in Japanese subjects, our study identified that the *AFF1* locus was significantly associated with SLE susceptibility.

As well as the identification of the novel SLE susceptibility locus, we observed significant replications of associations in the previously reported susceptibility loci. The replications were especially enriched in the loci identified through the studies in Asian populations, compared to those in European populations. Considering the ethnical heterogeneities in the epidemiology of SLE [19,20], these observations suggest the similarities in the genetic backgrounds of SLE shared within Asian populations, and also the existence of the both common and divergent genetic backgrounds encompassed between European and Asian populations.

Table 1. Results of a genome-wide association study for Japanese patients with SLE.

rsID[a]	Chr	Position (bp)	Cytoband	Gene	Allele[b]	No. subjects		Allele 1 freq.		OR (95%CI)	*P*
					1/2	Case	Control	Case	Control		
rs10168266	2	191,644,049	2q32	*STAT4*	T/C	891	3,384	0.37	0.27	1.59 (1.42–1.78)	2.7×10^{-16}
rs9501626	6	32,508,322	6p21	HLA region	A/C	891	3,381	0.20	0.12	1.86 (1.62–2.13)	1.0×10^{-18}
rs2230926	6	138,237,759	6q23	*TNFAIP3*	G/T	891	3,377	0.11	0.069	1.75 (1.47–2.08)	1.9×10^{-10}
rs6964720	7	75,018,280	7q11	*HIP1*	G/A	891	3,384	0.25	0.19	1.43 (1.27–1.63)	1.3×10^{-8}
rs2254546	8	11,381,089	8p23	*BLK*	G/A	891	3,384	0.78	0.72	1.42 (1.61–1.25)	4.1×10^{-8}
rs6590330	11	127,816,269	11q24	*ETS1*	A/G	891	3,368	0.48	0.39	1.44 (1.30–1.60)	1.3×10^{-11}

[a]SNPs that satisfied the threshold of $P<5.0\times10^{-8}$ were indicated.
[b]Based on forward strand of NCBI Build 36.3.
SLE, systemic lupus erythematosus; OR, odds ratio.
doi:10.1371/journal.pgen.1002455.t001

To effectively detect the novel SLE susceptibility locus, we integrated cis-eQTL effects of the SNPs and prioritized the results of the GWAS. In addition to identifying a novel locus for SLE-susceptibility, our study demonstrated approximately 30% of confirmed SLE-susceptibility loci were comprised of cis-eQTLs. We also confirmed cis-regulatory effect of the landmark SNP in the *AFF1* locus, rs340630, on *AFF1* transcripts, which had been prioritized through the eQTL study. These results would suggest that accumulation of quantitative changes in gene expression would accelerate the disease onset of SLE. It would also demonstrate the validity of applying eQTL study in the search of the susceptible genes for SLE or other autoimmune diseases, as previously suggested in the study for celiac disease [24]. To our knowledge, this is one of the initial studies to successfully discover a new locus by prioritizing GWAS results using eQTLs, and should contribute to the approaches assessing genetic loci still being uncaptured by recent large-scaled GWASs due to stringent significance threshold for multiple hypothesis testing [21].

We observed prominent expression levels of *AFF1* in $CD4^+$ and $CD19^+$ peripheral blood lymphocytes, which would imply an important role for *AFF1* in helper-T-cells and B-cells. In fact, *AFF1* is essential for normal lymphocyte development, as demonstrated in mice deficient for *AFF1*; severe reduction were observed in the thymic double positive CD4/CD8 population and the bone marrow pre-B and mature B-cell numbers [32]. The risk A allele of rs340630 demonstrated a cis-eQTL effect on the *AFF1* transcript with enhanced expression levels. As the *AFF1* locus was also demonstrated as an eQTL in primary liver cells [33], the cis-regulatory effect may hold in primary cells as well as lymphoblastoid cells used in the present study. However, because the mechanism of transcriptional regulation is substantially different among cell types [34], cell-type specific analyses including those for primary T-cells and B-cells are needed for understanding the precise role of *AFF1* variant in primary lymphocytes. Although further functional investigation is necessary, our observation suggested that *AFF1* is involved in the etiology of SLE through the regulation of development and activity of lymphocytes. It is of note that *AFF3*, which also belongs to the AF4/FMR2 family, is associated with susceptibility to autoimmune diseases [35].

One of our study's limitations is the selection of SNPs for the replication study using the results of the pooled DNA approach [30], which used a different genotyping platform from that of the present GWAS. Moreover, the association signals based on Silhouette scores in pooled analysis would be less reliable compared to those based on individual genotyping. Since direct comparisons of the association signals of the same single SNPs between the studies would be difficult due to these issues, we adopted the complementary approach that referred the association signals of the multiple SNPs in the pooled analysis for each of the single SNPs in the GWAS, taking account of LD and physical distances between the SNPs. However, there would exist a possibility that the variant(s) truly associated with SLE was left not to be examined in the replication study. It should be noted that only 1 SNP among the 8 selected SNPs yielded the significant association with SLE, although further enrichments of the significant associations might be anticipated. To elucidate effectiveness and limitation of our approach, further assessments of the studies on the remaining loci would be desirable. It should also be noted that the control-case ratio of the subjects were relatively high in the replication study 2 (= 33.8), and this disproportionate ratio could have induced potential bias on the results of the association analysis of the SNPs. However, considering the homogeneous ancestries of the Japanese population [27] and that principal component analysis did not demonstrate significant population stratification in the control subjects of the replication study 2 (data not shown), the bias owing to population stratification might not be substantial.

In summary, through a GWAS and multi-staged replication studies in a Japanese population integrating eQTL study, our study identified *AFF1* as a novel susceptibility locus for SLE.

Materials and Methods

Subjects

We enrolled 2,278 systemic lupus erythematosus (SLE) cases and 31,948 controls. SLE cases enrolled in the genome-wide association study (GWAS) ($n = 891$) or part of the 2nd replication study ($n = 83$) were collected from 12 medical institutes in Japan under the support of the autoimmune disease study group of Research in Intractable Diseases, Japanese Ministry of Health, Labor and Welfare: Hokkaido University Graduate School of Medicine, Tohoku University Graduate School of Medicine, the University of Tokyo, Keio University School of Medicine, Juntendo University School of Medicine, University of Occupational and Environmental Health, University of Tsukuba, Tokyo Medical and Dental University, National Center for Global Health and Medicine, Nagasaki University, Wakayama Medical University, and Jichi Medical University. SLE cases ($n = 562$) and controls ($n = 653$) enrolled in the 1st replication study were collected from Kyushu University. Some of the SLE cases ($n = 742$) and controls ($n = 27,911$) enrolled in the 2nd replication study were collected from Kyoto University, Tokyo Women's

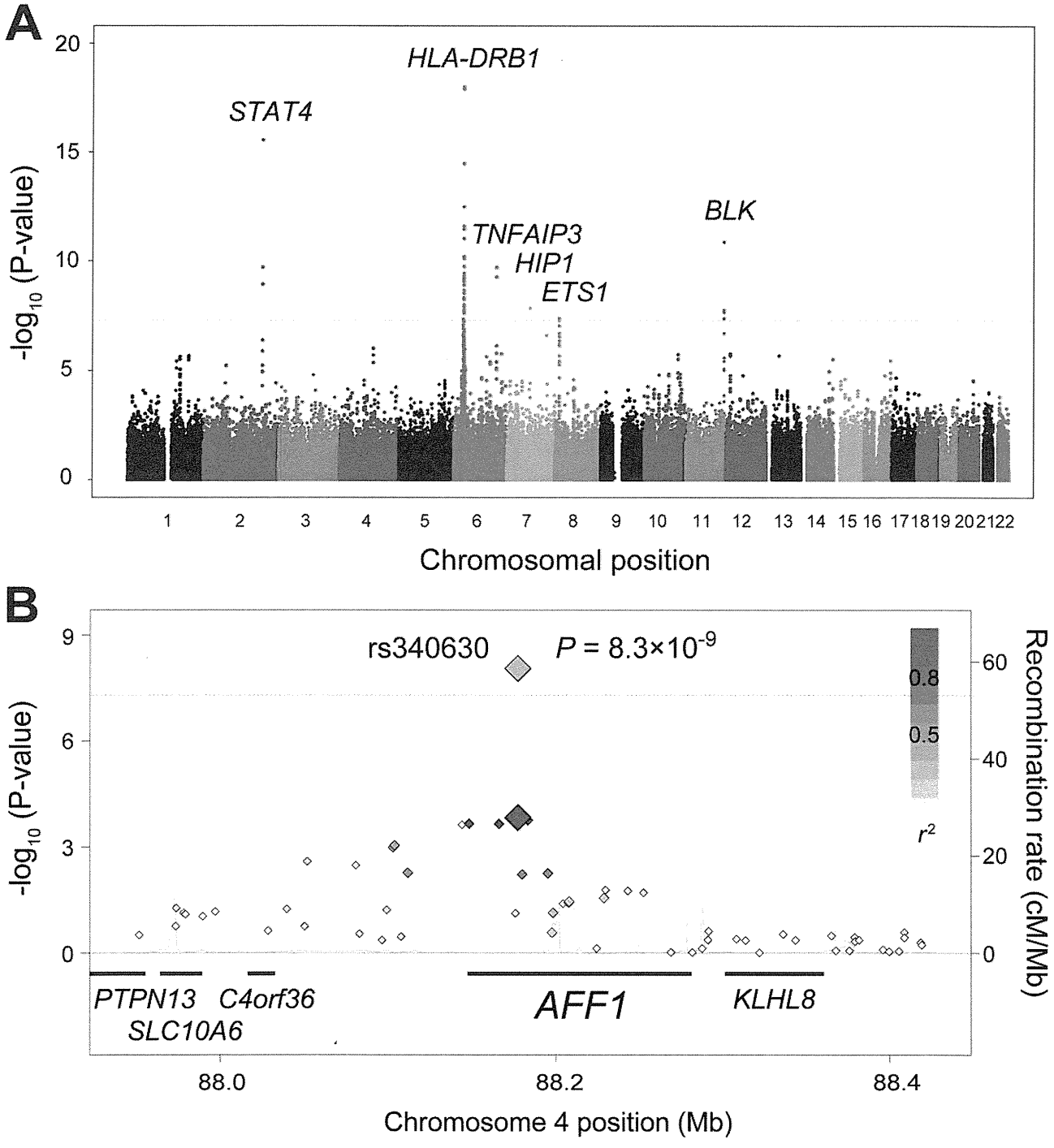

Figure 2. Associations of the *AFF1* locus with SLE. (A) A chromosomal plot of *P*-values in GWAS for SLE. (B) A regional plot in the *AFF1* locus. Diamond-shaped data points represent $-\log_{10}$ (*P*-values) of the SNPs. Large-sized points indicate the *P*-values of the landmark SNP, rs340630 (green for the combined study and red for the GWAS). Density of red color represents r^2 values with rs340630. Blue line represents recombination rates. Lower part indicates RefSeq genes. Gray dashed horizontal lines represent the threshold of $P = 5.0 \times 10^{-8}$. The plots were drawn using SNAP, version 2.1 [47].
doi:10.1371/journal.pgen.1002455.g002

Medical University, the University of Tokyo, and the BioBank Japan Project [36]. All subjects were of Japanese origin and provided written informed consent. SLE cases met the revised American College of Rheumatology (ACR) criteria for SLE [37]. Control subjects were confirmed to be free of autoimmune disease. Some of the SLE cases were included in our previous studies [38–40]. Details of the subjects are summarized in Table S1 and S2. This research project was approved by the ethical committees of the University of Tokyo, RIKEN, and affiliated medical institutes.

Table 2. Associations among previously reported SLE-related loci.

rsID	Chr	Position (bp)	Cytoband	Gene	Allele[a]	Allele 1 freq.		OR (95%CI)	*P*	eQTL[b]	Identified by the studies in[c]	
					1/2	Case	Control				Caucasians	Asians
rs2205960	1	171,458,098	1q25	*TNFSF4*	T/G	0.23	0.18	1.35 (1.19–1.54)	3.0×10^{-6}		+	
rs3024505	1	205,006,527	1q32	*IL10*	A/G	0.019	0.014	1.34 (0.90–2.00)	0.15		+	
rs13385731	2	33,555,394	2p22	*RASGRP3*	C/T	0.90	0.87	1.37 (1.15–1.64)	6.0×10^{-4}	+		+
rs10168266	2	191,644,049	2q32	*STAT4*	T/C	0.37	0.27	1.59 (1.42–1.78)	2.7×10^{-16}		+	
rs6445975	3	58,345,217	3p14	*PXK*	G/T	0.25	0.23	1.09 (0.96–1.23)	0.18	+	+	
rs10516487	4	102,970,099	4q24	*BANK1*	G/A	0.91	0.89	1.28 (1.07–1.53)	0.0070		+	
rs10036748	5	150,438,339	5q33	*TNIP1*	T/C	0.75	0.72	1.16 (1.03–1.31)	0.014			+
rs9501626	6	32,508,322	6p21	*HLA-DRB1*	A/C	0.20	0.12	1.86 (1.62–2.13)	1.0×10^{-18}		+	
rs548234	6	106,674,727	6q21	*PRDM1*	C/T	0.40	0.34	1.30 (1.16–1.44)	2.3×10^{-6}	+	+	
rs2230926	6	138,237,759	6q23	*TNFAIP3*	G/T	0.11	0.069	1.75 (1.47–2.08)	1.9×10^{-10}	+	+	
rs849142	7	28,152,416	7p15	*JAZF1*	C/T	0.999	0.999	2.72 (0.25–29.8)	0.41		+	
rs4917014	7	50,276,409	7p12	*IKZF1*	T/G	0.58	0.53	1.24 (1.11–1.38)	8.1×10^{-5}			+
rs6964720	7	75,018,280	7q11	*HIP1*	G/A	0.25	0.19	1.43 (1.27–1.62)	1.3×10^{-8}			+
rs4728142	7	128,361,203	7q32	*IRF5*	A/G	0.16	0.11	1.48 (1.28–1.72)	2.4×10^{-7}	+	+	
rs2254546	8	11,381,089	8p23	*BLK*	G/A	0.78	0.72	1.42 (1.25–1.61)	4.1×10^{-8}	+	+	
rs1913517	10	49,789,060	10q11	*WDFY4*	A/G	0.32	0.28	1.20 (1.07–1.35)	0.0013			+
rs4963128	11	579,564	11p15	*KIAA1542*	T/C	0.98	0.97	1.58 (1.03–2.44)	0.038	+	+	
rs2732552	11	35,041,168	11p13	*PDHX, CD44*	T/C	0.75	0.73	1.13 (1.00–1.27)	0.056		+	
rs4639966	11	118,078,729	11q23	Intergenic	T/C	0.32	0.28	1.22 (1.09–1.36)	7.3×10^{-4}			+
rs6590330	11	127,816,269	11q24	*ETS1*	A/G	0.48	0.39	1.44 (1.30–1.60)	1.3×10^{-11}			+
rs1385374	12	127,866,647	12q24	*SLC15A4*	T/C	0.19	0.16	1.21 (1.06–1.38)	0.0057			+
rs7329174	13	40,456,110	13q14	*ELF1*	G/A	0.30	0.25	1.32 (1.18–1.49)	2.2×10^{-6}			+
rs7197475	16	30,550,368	16p11	Intergenic	T/C	0.12	0.10	1.20 (1.02–0.41)	0.031			+
rs11150610	16	31,241,737	16p11	*ITGAM*	C/A	0.20	0.19	1.07 (0.94–1.22)	0.32	+	+	
rs12949531	17	13,674,531	17p12	Intergenic	T/C	0.28	0.27	1.02 (0.91–1.15)	0.73		+	
rs463426	22	20,139,185	22q11	*HIC2,UBE2L3*	T/C	0.52	0.48	1.20 (1.08–1.33)	6.1×10^{-4}		+	

[a]Based on forward strand of NCBI Build 36.3.
[b]Defined using gene expression data measured in lymphoblastoid B cell lines [28].
[c]Based on the previously reported studies for SLE susceptibility loci [3–18].
SLE, systemic lupus erythematosus; OR, odds ratio; eQTL, expression quantitative trait locus; GWAS, genome-wide association study.
doi:10.1371/journal.pgen.1002455.t002

Genotyping and quality control

In GWAS, 946 SLE cases and 3,477 controls were genotyped using Illumina HumanHap610-Quad and Illumina HumanHap550v3 Genotyping BeadChips (Illumina, CA, USA), respectively. After the exclusion of 47 SLE cases and 92 controls with call rates <0.98, SNPs with call rates <0.99 in SLE cases or controls,

Table 3. Results of combined study for Japanese patients with SLE.

rsID	Chr	Position (bp)	Cytoband	Gene	Allele	Stage	No. subjects		Allele 1 freq.		OR (95%CI)	*P*	eQTL[a]
					1/2		Case	Control	Case	Control			
rs340630	4	88,177,419	4q21	*AFF1*	A/G	GWAS	891	3,383	0.56	0.51	1.22 (1.10–1.36)	1.5×10^{-4}	+
						Replication study 1	550	646	0.57	0.49	1.40 (1.19–1.64)	4.6×10^{-5}	
						Replication study 2	820	27,911	0.56	0.53	1.14 (1.03–1.26)	0.0094	
						Combined study	2,261	31,940	0.56	0.52	1.21 (1.14–1.30)	8.3×10^{-9}	

[a]Defined using gene expression data measured in lymphoblastoid B cell lines [28].
doi:10.1371/journal.pgen.1002455.t003

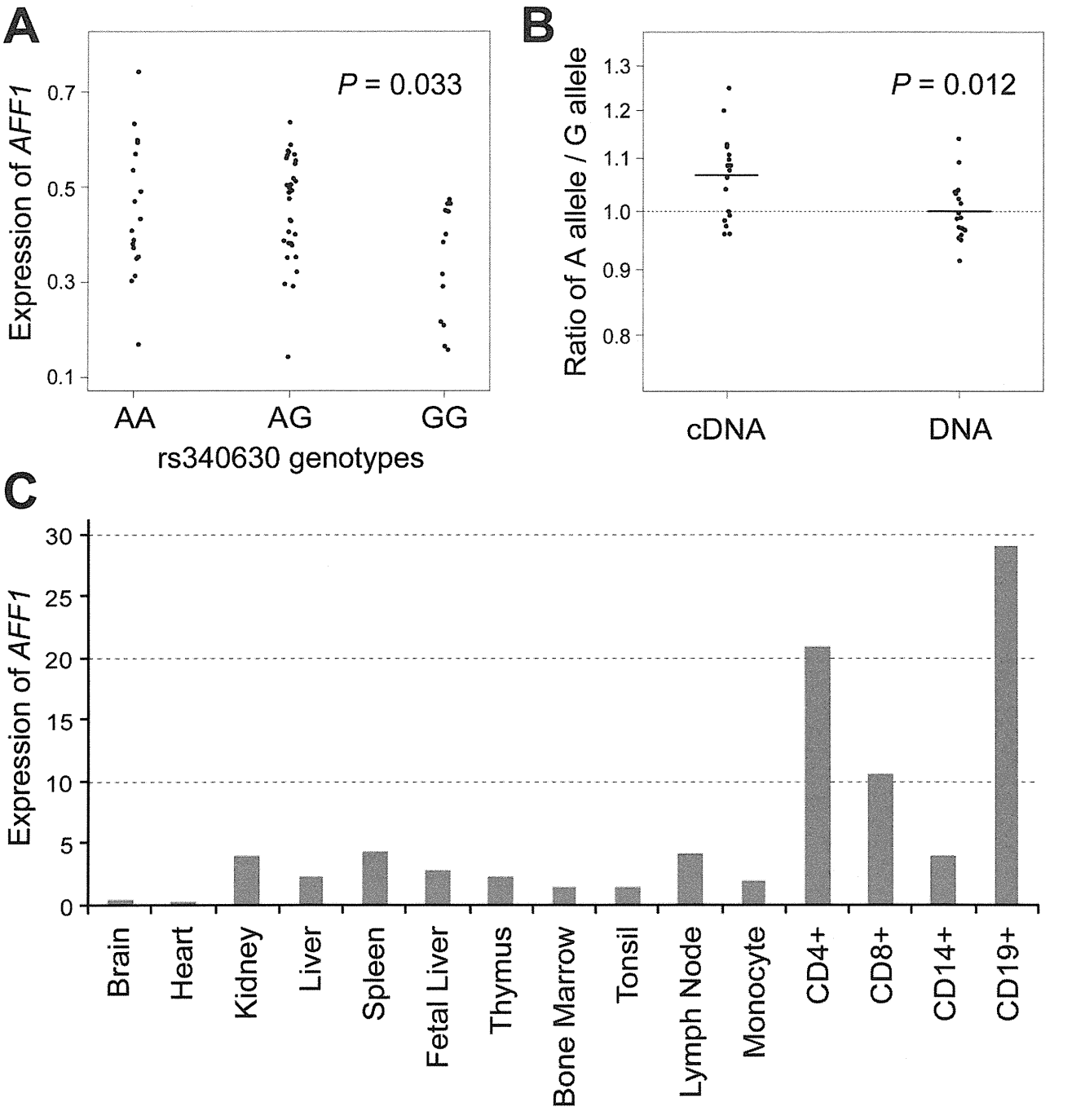

Figure 3. Association of rs340630 with *AFF1* expression. (A) Correlation between rs340630 genotypes and transcript levels of *AFF1* (NM_001166693) in EBV-transfected cell lines ($n = 62$) stimulated with PMA. (B) Allele-specific quantification (ASTQ) of *AFF1* transcripts. Allele specific-probes for rs340638 were used for quantification by qPCR. The ratios of A allele over G allele for the amounts of both cDNAs and DNAs were plotted in log scale for each cell line. (C) *AFF1* expression in various tissues. Transcripts levels of *AFF*1 were quantified by qPCR and were normalized by *GAPDH* levels.
doi:10.1371/journal.pgen.1002455.g003

non-autosomal SNPs, and SNPs not shared between SLE cases and controls, were excluded. We excluded 7 closely related SLE cases in a 1st or 2nd degree of kinship based on identity-by-descent estimated using PLINK version 1.06 [41]. We then excluded 1 SLE cases and 1 controls whose ancestries were estimated to be distinct from East-Asian populations using PCA performed along with the genotype data of Phase II HapMap populations (release 24) [29] using EIGENSTRAT version 2.0 [42]. Subsequently, SNPs with minor allele frequencies <0.01 in SLE cases or controls, SNPs with exact *P*-values of Hardy-Weinberg equilibrium test $<1.0\times10^{-6}$ in controls, or SNPs with ambiguous cluster plots were excluded. Finally, 430,797 SNPs for 891 SLE cases and 3,384 controls were obtained. Genotyping of SNPs in replication studies was performed using TaqMan Assay or Illumina HumanHap610-Quad Genotyping BeadChip (Illumina, CA, USA).

Association analysis of the SNPs

Association of SNPs in GWAS and replication studies were tested with Cochran-Armitage's trend test. Combined analysis was performed with Mantel-Haenzel method. Associations of previously reported SLE susceptibility loci [3–18] were evaluated using the results of the GWAS. Genotype imputation was performed for non-genotyped SNPs using MACH version 1.0 [43] with Phase II HapMap East-Asian individuals as references [29], as previously described [44]. All imputed SNPs demonstrated imputation scores, *Rsq*, >0.70.

eQTL study

We analyzed gene expression data previously measured in lymphoblastoid B cell lines from Phase II HapMap East-Asian individuals using Illumina's human whole-genome expression array (WG-6 version 1) (accession number; GSE6536) [28]. Expression data were normalized across the individuals. We used BLAST to map 47,294 Illumina array probes onto human autosomal reference genome sequences (Build 36). We discarded probes mapped with expectation values smaller than 0.01 to multiple loci, or for which there was polymorphic HapMap SNP(s) inside the probe. Then, 19,047 probes with exact matches to a unique locus with 100% identity and with a mean signal intensity greater than background were obtained. Genotype data of HapMap individuals were obtained for SNPs included in the GWAS. Associations of SNP genotypes (coded as 0, 1, and 2) with expression levels of each of the cis-eQTL probes (located within ±300 kbp regions of the SNPs) were evaluated using linear regression assuming additive effects of the genotypes on the expression levels. Considering the significant overlap between eQTL and genetic loci responsible for autoimmune diseases [24], we applied relatively less stringent multiple testing threshold of FDR *Q*-values<0.2 for the definition of eQTL. SNPs that exhibited this threshold with any of the corresponding cis-eQTL probes were denoted as eQTL positive.

Selection of SNPs enrolled in the replication studies

In order to select SNPs for further replication studies, we firstly integrated the results of GWAS and eQTL study. SNPs that satisfied $P<1.0\times10^{-4}$ in GWAS, or the SNPs that satisfied $1.0\times10^{-4}\leq P<1.0\times10^{-3}$ in GWAS and denoted as eQTL positive, were selected. Among these, SNPs most significantly associated in each of the genomic loci and not included in the previously reported SLE susceptibility loci [3–18] were further evaluated.

Then, the results of the concurrently proceeding genome-wide scan for SLE in the Japanese subjects using a pooled DNA approach were referred (Tahira T et al. Presented at the 59th Annual Meeting of the American Society of Human Genetics, October 21, 2009). In the scan, DNA collected from 447 SLE cases and 680 controls of Japanese origin were pooled respectively, and genotyped using GeneChip Human Mapping 500K Array Set (Affymetrix, CA, USA). SNPs were ranked according to the Silhouette scores estimated based on relative allele scores (RAS) between SLE cases and controls, and rank-based *P*-values were assigned [30]. By referring to association signals in multiple neighboring SNPs in the pooled analysis, we selected SNPs for replication study 1. Namely, if the SNP of interest was in LD ($r^2>0.5$) or was located within ±100 kbp of SNPs showing association signals in the pooled analysis (rank-based $P<0.01$), it would be selected. SNPs that satisfied $P<1.0\times10^{-6}$ in the combined study of GWAS and replication study 1 were further evaluated in replication study 2 (Figure 1).

Quantification of *AFF1* expression

EBV-transformed lymphoblastoid cell lines ($n=62$) were established by Pharma SNP Consortium (Tokyo, Japan) using peripheral blood lymphocytes of Japanese healthy individuals. Cells were incubated for 2 h in medium alone (RPMI 1640 medium containing 10% FBS, 1% penicillin, and 1% streptomycin) or with 100 ng/ml PMA. Conditions for cell stimulation were optimized before the experiment as previously described [45]. Cells were then harvested and total RNA was isolated using an RNeasy Mini Kit (Qiagen) with DNase treatment. Total RNA (1 μg) was reverse transcribed using TaqMan Gold RT-PCR reagents with random hexamers (Applied Biosystems). Real-time quantitative PCR was performed in triplicate using an ABI PRISM 7900 and TaqMan gene expression assays (Applied Biosystems). Specific probes (Hs01089428_m1) for transcript of *AFF1* (NM_001166693) were used. Expression of *AFF1* in various tissues was also quantified using Premium Total RNA (Clontech). The data were normalized to *GAPDH* levels. *GUS* levels were also evaluated for internal control, and similar results were obtained. Correlation coefficient, R^2, between rs340630 genotypes and transcript levels of *AFF1* was evaluated.

Allele-specific transcript quantification (ASTQ)

ASTQ of *AFF1* in PSC cells was performed as previously described [46]. DNAs were extracted by using a DNeasy Kit (QIAGEN). RNA extraction and cDNA preparation were performed as described above. For PSC cells ($n=17$) that were heterozygous for both rs340630 (the landmark SNP of GWAS) and rs340638 (located in the 5′-untranslated region of *AFF1* and in absolute LD with rs340630), expression levels of *AFF1* were quantified by qPCR on an ABI Prism 7900 using a custom-made TaqMan MGB-probe set for rs340638. Primer sequences were 5′-CTAACTGTGGCCCGCGTTG-3′ and 5′-CCCGGCGCA-GTTTCTGAG-3′. The probe sequences were 5′-VIC-CGAA-GACCGCCAGCGCCCAAC-TAMRA-3′ and 5′-FAM-CGAA-GACCGCCGGCGCCCAA-TAMRA-3′. Ct values of VIC and FAM were obtained for genomic DNA and cDNA samples after 40 cycles of real-time PCR. We also prepared genomic DNA of samples homozygous for each allele and mixed them at different ratios (2:8, 3:7, 4:6, 5:5, 6:4, 7:3, 8:2) to create a standard curve by plotting Ct values of VIC/FAM against the allelic ratio of VIC/FAM for each mixture. Using the standard curve, we calculated the allelic ratios for each genomic DNA and cDNA samples. We measured each sample in quadruplicate in one assay; tests were independently repeated twice.

Web resources

The URLs for data presented herein are as follows.

NCBI GEO, http://www.ncbi.nlm.nih.gov/geo

BioBank Japan Project, http://biobankjp.org

PLINK software, http://pngu.mgh.harvard.edu/~purcell/plink/index.shtml

International HapMap Project, http://www.hapmap.org

EIGENSTRAT software, http://genepath.med.harvard.edu/~reich/Software.htm

MACH and mach2qtl software, http://www.sph.umich.edu/csg/abecasis/MACH/index.html

SNAP, http://www.broadinstitute.org/mpg/snap/index.php

Supporting Information

Figure S1 Principal component analysis (PCA) plot of the subjects. PCA plot of subjects enrolled in the GWAS for SLE. SLE cases and the controls enrolled in the GWAS are plotted based on

eigenvectors 1 and 2 obtained from the PCA using EIGENSTRAT version 2.0 [42], along with European (CEU), African (YRI), Japanese (JPT), and Chinese (CHB) individuals obtained from the Phase II HapMap database (release 22) [29]. Subjects who were estimated to be outliers in terms of ancestry from East-Asian (JPT+CHB) clusters and excluded from the study are indicated by black arrows.
(TIF)

Figure S2 Quantile-Quantile plot (QQ-plot) of *P*-values in the GWAS for SLE. The horizontal axis indicates the expected $-\log_{10}$ (*P*-values). The vertical axis indicates the observed $-\log_{10}$ (*P*-values). The QQ-plot for the *P*-values of all SNPs that passed the quality control criteria is indicated in blue. The QQ-plot for the *P*-values after the removal of SNPs included in the previously reported SLE susceptibility loci is indicated in black. The gray line represents $y = x$. The SNPs for which the *P*-value was smaller than 1.0×10^{-15} are indicated at the upper limit of the plot.
(TIF)

Table S1 Basal characteristics of cohorts.
(DOC)

Table S2 Frequency of clinical characteristics of SLE in this GWAS.
(DOC)

Table S3 Distributions of eQTL positivity rates of the SNPs.
(DOC)

Table S4 Results of replication study 1 for Japanese patients with SLE.
(DOC)

Table S5 Results of replication studies 1 and 2 for Japanese patients with SLE.
(DOC)

Acknowledgments

We are grateful to Dr. A. Miyatake, the members of the Rotary Club of Osaka-Midosuji District 2660 Rotary International in Japan, the autoimmune disease study group, and the staffs of the BioBank Japan Project for supporting the study and clinical sample collection. We thank the members of the Laboratory for Autoimmune Diseases, CGM, RIKEN, for their assistance.

Author Contributions

Conceived and designed the experiments: Y. Okada, K. Shimane, Y. Kochi, A. Suzuki, M. Kubo, N. Kamatani, R. Yamada, Y. Nakamura, K. Yamamoto. Performed the experiments: Y. Kochi, N. Hosono, M. Kubo, K. Myouzen, T. Horiuchi, T. Tahira, K. Hayashi. Analyzed the data: Y. Okada, A. Takahashi, T. Tsunoda, K. Higasa, R. Yamada. Contributed reagents/materials/analysis tools: T. Horita, T. Atsumi, T. Koike, T. Ishii, A. Okamoto, K. Fujio, M. Hirakata, H. Amano, Y. Takasaki, Y. Kondo, S. Ito, T. Sumida, K. Takada, A. Mimori, K. Saito, Y. Tanaka, M. Kamachi, N. Nishimoto, Y. Kawaguchi, C. Terao, K. Ohmura, T. Mimori, F. Matsuda, O.W. Mohammed, K. Matsuda, K. Shimane, K. Ikari, H. Yamanaka. Wrote the paper: Y. Okada, K. Shimane, Y. Kochi, A. Suzuki, R. Yamada, K. Yamamoto.

References

1. Lipsky PE (2001) Systemic lupus erythematosus: an autoimmune disease of B cell hyperactivity. Nat Immunol 2: 764–766.
2. Sestak AL, Shaver TS, Moser KL, Neas BR, Harley JB (1999) Familial aggregation of lupus and autoimmunity in an unusual multiplex pedigree. J Rheumatol 26: 1495–1499.
3. Sigurdsson S, Nordmark G, Goring HH, Lindroos K, Wiman AC, et al. (2005) Polymorphisms in the tyrosine kinase 2 and interferon regulatory factor 5 genes are associated with systemic lupus erythematosus. Am J Hum Genet 76: 528–537.
4. Graham RR, Kozyrev SV, Baechler EC, Reddy MV, Plenge RM, et al. (2006) A common haplotype of interferon regulatory factor 5 (IRF5) regulates splicing and expression and is associated with increased risk of systemic lupus erythematosus. Nat Genet 38: 550–555.
5. Graham RR, Kyogoku C, Sigurdsson S, Vlasova IA, Davies LR, et al. (2007) Three functional variants of IFN regulatory factor 5 (IRF5) define risk and protective haplotypes for human lupus. Proc Natl Acad Sci U S A 104: 6758–6763.
6. Remmers EF, Plenge RM, Lee AT, Graham RR, Hom G, et al. (2007) STAT4 and the risk of rheumatoid arthritis and systemic lupus erythematosus. N Engl J Med 357: 977–986.
7. Cunninghame Graham DS, Graham RR, Manku H, Wong AK, Whittaker JC, et al. (2008) Polymorphism at the TNF superfamily gene TNFSF4 confers susceptibility to systemic lupus erythematosus. Nat Genet 40: 83–89.
8. Nath SK, Han S, Kim-Howard X, Kelly JA, Viswanathan P, et al. (2008) A nonsynonymous functional variant in integrin-alpha(M) (encoded by ITGAM) is associated with systemic lupus erythematosus. Nat Genet 40: 152–154.
9. Harley JB, Alarcon-Riquelme ME, Criswell LA, Jacob CO, Kimberly RP, et al. (2008) Genome-wide association scan in women with systemic lupus erythematosus identifies susceptibility variants in ITGAM, PXK, KIAA1542 and other loci. Nat Genet 40: 204–210.
10. Kozyrev SV, Abelson AK, Wojcik J, Zaghlool A, Linga Reddy MV, et al. (2008) Functional variants in the B-cell gene BANK1 are associated with systemic lupus erythematosus. Nat Genet 40: 211–216.
11. Hom G, Graham RR, Modrek B, Taylor KE, Ortmann W, et al. (2008) Association of systemic lupus erythematosus with C8orf13-BLK and ITGAM-ITGAX. N Engl J Med 358: 900–909.
12. Graham RR, Cotsapas C, Davies L, Hackett R, Lessard CJ, et al. (2008) Genetic variants near TNFAIP3 on 6q23 are associated with systemic lupus erythematosus. Nat Genet 40: 1059–1061.
13. Musone SL, Taylor KE, Lu TT, Nititham J, Ferreira RC, et al. (2008) Multiple polymorphisms in the TNFAIP3 region are independently associated with systemic lupus erythematosus. Nat Genet 40: 1062–1064.
14. Han JW, Zheng HF, Cui Y, Sun LD, Ye DQ, et al. (2009) Genome-wide association study in a Chinese Han population identifies nine new susceptibility loci for systemic lupus erythematosus. Nat Genet 41: 1234–1237.
15. Gateva V, Sandling JK, Hom G, Taylor KE, Chung SA, et al. (2009) A large-scale replication study identifies TNIP1, PRDM1, JAZF1, UHRF1BP1 and IL10 as risk loci for systemic lupus erythematosus. Nat Genet 41: 1228–1233.
16. Yang W, Shen N, Ye DQ, Liu Q, Zhang Y, et al. (2010) Genome-wide association study in Asian populations identifies variants in ETS1 and WDFY4 associated with systemic lupus erythematosus. PLoS Genet 6: e1000841. doi:10.1371/journal.pgen.1000841.
17. Lessard CJ, Adrianto I, Kelly JA, Kaufman KM, Grundahl KM, et al. (2011) Identification of a systemic lupus erythematosus susceptibility locus at 11p13 between PDHX and CD44 in a multiethnic study. Am J Hum Genet 88: 83–91.
18. Yang J, Yang W, Hirankarn N, Ye DQ, Zhang Y, et al. (2011) ELF1 is associated with systemic lupus erythematosus in Asian populations. Hum Mol Genet 20: 601–607.
19. Hopkinson ND, Doherty M, Powell RJ (1994) Clinical features and race-specific incidence/prevalence rates of systemic lupus erythematosus in a geographically complete cohort of patients. Ann Rheum Dis 53: 675–680.
20. Danchenko N, Satia JA, Anthony MS (2006) Epidemiology of systemic lupus erythematosus: a comparison of worldwide disease burden. Lupus 15: 308–318.
21. Yang J, Benyamin B, McEvoy BP, Gordon S, Henders AK, et al. (2010) Common SNPs explain a large proportion of the heritability for human height. Nat Genet 42: 565–569.
22. Raychaudhuri S, Plenge RM, Rossin EJ, Ng AC, Purcell SM, et al. (2009) Identifying relationships among genomic disease regions: predicting genes at pathogenic SNP associations and rare deletions. PLoS Genet 5: e1000534. doi:10.1371/journal.pgen.1000534.
23. Cantor RM, Lange K, Sinsheimer JS (2010) Prioritizing GWAS results: A review of statistical methods and recommendations for their application. Am J Hum Genet 86: 6–22.
24. Dubois PC, Trynka G, Franke L, Hunt KA, Romanos J, et al. (2010) Multiple common variants for celiac disease influencing immune gene expression. Nat Genet 42: 295–302.
25. Cookson W, Liang L, Abecasis G, Moffatt M, Lathrop M (2009) Mapping complex disease traits with global gene expression. Nat Rev Genet 10: 184–194.
26. Kochi Y, Okada Y, Suzuki A, Ikari K, Terao C, et al. (2010) A regulatory variant in CCR6 is associated with rheumatoid arthritis susceptibility. Nat Genet 42: 515–519.
27. Yamaguchi-Kabata Y, Nakazono K, Takahashi A, Saito S, Hosono N, et al. (2008) Japanese population structure, based on SNP genotypes from 7003 individuals compared to other ethnic groups: effects on population-based association studies. Am J Hum Genet 83: 445–456.
28. Stranger BE, Nica AC, Forrest MS, Dimas A, Bird CP, et al. (2007) Population genomics of human gene expression. Nat Genet 39: 1217–1224.
29. The International HapMap Consortium (2003) The International HapMap Project. Nature 426: 789–796.

30. Pearson JV, Huentelman MJ, Halperin RF, Tembe WD, Melquist S, et al. (2007) Identification of the genetic basis for complex disorders by use of pooling-based genomewide single-nucleotide-polymorphism association studies. Am J Hum Genet 80: 126–139.
31. Xia ZB, Popovic R, Chen J, Theisler C, Stuart T, et al. (2005) The MLL fusion gene, MLL-AF4, regulates cyclin-dependent kinase inhibitor CDKN1B (p27kip1) expression. Proc Natl Acad Sci U S A 102: 14028–14033.
32. Isnard P, Core N, Naquet P, Djabali M (2000) Altered lymphoid development in mice deficient for the mAF4 proto-oncogene. Blood 96: 705–710.
33. Schadt EE, Molony C, Chudin E, Hao K, Yang X, et al. (2008) Mapping the genetic architecture of gene expression in human liver. PLoS Biol 6: e107. doi:10.1371/journal.pbio.0060107.
34. Ernst J, Kheradpour P, Mikkelsen TS, Shoresh N, Ward LD, et al. (2011) Mapping and analysis of chromatin state dynamics in nine human cell types. Nature 473: 43–49.
35. Stahl EA, Raychaudhuri S, Remmers EF, Xie G, Eyre S, et al. (2010) Genome-wide association study meta-analysis identifies seven new rheumatoid arthritis risk loci. Nat Genet 42: 508–514.
36. Nakamura Y (2007) The BioBank Japan Project. Clin Adv Hematol Oncol 5: 696–697.
37. Hochberg MC (1997) Updating the American College of Rheumatology revised criteria for the classification of systemic lupus erythematosus. Arthritis Rheum 40: 1725.
38. Suzuki A, Yamada R, Kochi Y, Sawada T, Okada Y, et al. (2008) Functional SNPs in CD244 increase the risk of rheumatoid arthritis in a Japanese population. Nat Genet 40: 1224–1229.
39. Shimane K, Kochi Y, Horita T, Ikari K, Amano H, et al. (2010) The association of a nonsynonymous single-nucleotide polymorphism in TNFAIP3 with systemic lupus erythematosus and rheumatoid arthritis in the Japanese population. Arthritis Rheum 62: 574–579.
40. Myouzen K, Kochi Y, Shimane K, Fujio K, Okamura T, et al. (2010) Regulatory polymorphisms in EGR2 are associated with susceptibility to systemic lupus erythematosus. Hum Mol Genet 19: 2313–2320.
41. Purcell S, Neale B, Todd-Brown K, Thomas L, Ferreira MA, et al. (2007) PLINK: a tool set for whole-genome association and population-based linkage analyses. Am J Hum Genet 81: 559–575.
42. Price AL, Patterson NJ, Plenge RM, Weinblatt ME, Shadick NA, et al. (2006) Principal components analysis corrects for stratification in genome-wide association studies. Nat Genet 38: 904–909.
43. Li Y, Willer C, Sanna S, Abecasis G (2009) Genotype imputation. Annu Rev Genomics Hum Genet 10: 387–406.
44. Okada Y, Takahashi A, Ohmiya H, Kumasaka N, Kamatani Y, et al. (2011) Genome-wide association study for C-reactive protein levels identified pleiotropic associations in the IL6 locus. Hum Mol Genet 20: 1224–1231.
45. Aikawa Y, Yamamoto M, Yamamoto T, Morimoto K, Tanaka K (2002) An anti-rheumatic agent T-614 inhibits NF-kappaB activation in LPS- and TNF-alpha-stimulated THP-1 cells without interfering with IkappaBalpha degradation. Inflamm Res 51: 188–194.
46. Akamatsu S, Takata R, Ashikawa K, Hosono N, Kamatani N, et al. (2010) A functional variant in NKX3.1 associated with prostate cancer susceptibility down-regulates NKX3.1 expression. Hum Mol Genet 19: 4265–4272.
47. Johnson AD, Handsaker RE, Pulit SL, Nizzari MM, O'Donnell CJ, et al. (2008) SNAP: a web-based tool for identification and annotation of proxy SNPs using HapMap. Bioinformatics 24: 2938–2939.

Nonimmunoglobulin target loci of activation-induced cytidine deaminase (AID) share unique features with immunoglobulin genes

Lucia Kato[a], Nasim A. Begum[a], A. Maxwell Burroughs[b], Tomomitsu Doi[a,1], Jun Kawai[b], Carsten O. Daub[b], Takahisa Kawaguchi[c], Fumihiko Matsuda[c], Yoshihide Hayashizaki[b], and Tasuku Honjo[a,2]

[a]Department of Immunology and Genomic Medicine and [c]The Center for Genomic Medicine, Graduate School of Medicine, Kyoto University, Kyoto 606-8501, Japan; and [b]RIKEN Omics Science Center (OSC), RIKEN Yokohama Institute, Yokohama, Kanagawa 230-0045, Japan

Contributed by Tasuku Honjo, December 28, 2011 (sent for review December 5, 2011)

Activation-induced cytidine deaminase (AID) is required for both somatic hypermutation and class-switch recombination in activated B cells. AID is also known to target nonimmunoglobulin genes and introduce mutations or chromosomal translocations, eventually causing tumors. To identify as-yet-unknown AID targets, we screened early AID-induced DNA breaks by using two independent genome-wide approaches. Along with known AID targets, this screen identified a set of unique genes (*SNHG3, MALAT1, BCL7A,* and *CUX1*) and confirmed that these loci accumulated mutations as frequently as *Ig* locus after AID activation. Moreover, these genes share three important characteristics with the Ig gene: translocations in tumors, repetitive sequences, and the epigenetic modification of chromatin by H3K4 trimethylation in the vicinity of cleavage sites.

deep sequencing | end labeling by biotin oligonucleotide | microarray

Activation-induced cytidine deaminase (AID) is expressed in germinal center (GC) B cells upon antigen stimulation and is essential for two types of genetic alteration in the Ig gene: class switch recombination (CSR) and somatic hypermutation (SHM), which provide the genetic basis for antibody memory (1, 2). CSR produces antibodies with different effector functions by recombination at Ig heavy chain (H) switch (S) regions, so that the μ-chain constant (Cμ) region is replaced by a downstream C_H region. SHM introduces nontemplated point mutations in the rearranged variable (V) region genes, resulting in incremented antigen receptor affinity after clonal selection (3, 4).

Functional studies on AID mutants have shown that distinct AID domains are required for SHM and CSR, although AID has a single catalytic center (cytidine deaminase motif) in the middle of the molecule. Deletions and alterations in the N-terminal region affect both the CSR and SHM activities (5). However, AID C-terminal mutants almost completely lose CSR activity but retain or even increase SHM activity (6, 7). Although C-terminally truncated AID mutants cleave both V and S regions and induce enhanced c-myc-IgH translocations, they cannot mediate CSR, suggesting that the C-terminal domain is not required for DNA cleavage but is required to correctly pair cleaved ends (8).

The DNA cleavage of targets in CSR and SHM (the S region and V region, respectively) requires their transcription (9–12). Indeed, AID-induced mutations (SHM) are generally detected in a region within 2 kb downstream of the transcription start site (TSS) (13, 14). Transcription appears to play two roles in the targeting of cleavage sites. First, transcription is associated with the epigenetic marking of the target locus, particularly by H3K4 trimethylation (H3K4me3). The histone chaperone complex FACT is required to regulate H3K4me3 in the target S region, and FACT knockdown abolishes H3K4me3 and DNA cleavage in this region (15). Second, transcription is probably required to induce non-B structures in highly repetitive sequences such as S regions (16–18), due to excessive negative supercoiling induced immediately downstream of transcription. V regions have also been shown to form stem-loop structures under these conditions (19, 20). Non-B structure involvement has recently been reported in transcription-associated mutations in repetitive sequences such as the dinucleotide repeat hot spots or triplet repeat expansion/contractions causing Huntington's disease (17, 21, 22).

AID-dependent DNA cleavage is, in general, specific to the Ig locus. However, a number of reports have shown that AID can induce DNA cleavage in non-Ig loci. AID non-Ig targets were first demonstrated by studies on AID transgenic mice that produce numerous T lymphomas, in which vast numbers of mutations accumulate in the genes encoding the T-cell receptor, CD4, CD5, c-myc, and PIM1 (23, 24). This finding was followed by the observations that AID deficiency abolishes c-myc-Ig translocation and reduces the incidence of plasmacytoma (25, 26). AID expression is specific to activated B cells under normal conditions. However, AID expression has also been found in non-B cells, especially in cells stimulated by infection with pathogens such as human T-cell leukemia virus type 1 (HTLV1), hepatitis C virus (HCV), Epstein–Barr (EB) virus, and *Helicobacter pylori* (27–30). Based on these observations, AID is postulated to induce tumorigenesis, especially in B lymphomas and leukemias—and AID is expressed in many GC-derived human B-cell lymphomas (31–33). The prognosis of acute lymphocytic leukemia (ALL) and chronic myeloid leukemia (CML) is linked with AID expression (34, 35). It is therefore important to determine which non-Ig genes can be targeted by AID, and what features, if any, they share with Ig genes.

Several approaches have been used to explore AID non-Ig target genes in B cells. Candidate approaches involving the direct sequencing of proto-oncogenes, genes involved in translocations, or genes transcribed in normal GC B cells have shown that AID mutates several non-Ig genes, including *BCL6*, *MYC*, *PIM1*, and *PAX5* (24, 32, 36, 37). More recently, several efforts have been made to identify AID targets in a whole genome. These approaches have used chromatin immunoprecipitation (ChIP) of CSR-related proteins in combination with genome-wide tiling microarrays (ChIP-chip) or deep sequencing (ChIP-seq) on the assumption that proteins involved in CSR bind to AID targets. RPA, Nbs1, AID itself, and Spt5 have been used as marking proteins in this type of study (38–40). However, these approaches did not necessarily show that all of the protein-bound targets are cleaved or mutated by AID. There are indications that some genes identified by such approaches are not tran-

Author contributions: L.K., T.D., and T.H. designed research; L.K., N.A.B., and A.M.B. performed research; T.K. and F.M. contributed new reagents/analytic tools; L.K., N.A.B., A.M.B., J.K., C.O.D., and Y.H. analyzed data; and L.K. and T.H. wrote the paper.

The authors declare no conflict of interest.

[1]Present address: Laboratory Animal Research Center, Institute of Medical Science, University of Tokyo, 4-6-1 Shirokanedai, Minato-ku, Tokyo 108-8639, Japan.

[2]To whom correspondence should be addressed. E-mail: honjo@mfour.med.kyoto-u.ac.jp.

This article contains supporting information online at www.pnas.org/lookup/suppl/doi:10.1073/pnas.1120791109/-/DCSupplemental.

scribed (39). Therefore, it is important to reexamine non-Ig AID target genes by using a different strategy.

Here, we report four AID targets, identified by a combination of unique techniques. After directly labeling the DNA breakage ends from AID-induced cleavage with a biotinylated linker, we isolated the labeled fragments with streptavidin beads and analyzed them by a combination of promoter arrays and genome-wide sequencing. The candidates identified were then confirmed by quantitative PCR (qPCR) and the actual demonstration of mutations. With these methods, we identified at least four previously unknown AID targets—*SNHG3, MALAT1, BCL7A,* and *CUX1*. We found that these targets share important characteristics with Ig genes, namely, repetitive sequences that can form non-B structures upon efficient transcription, and the accumulation of H3K4me3 histone modifications on the chromatin.

Results

AID-Induced DNA Cleavage Detected by Labeling DNA Break Ends with a Biotinylated Linker. To detect genome-wide AID-induced DNA breaks, we used a modified in situ DNA end-labeling technique as described (8, 41) in BL2 cells, a Burkitt's lymphoma cell line that serves as an in vitro model for studying the SHM mechanism (31, 42, 43). We used the BL2 clone BL2-ΔC-AIDER, which expresses JP8Bdel, an AID mutant lacking the C-terminal 16 residues, fused with the hormone-binding domain of the estrogen receptor (ER) (JP8Bdel-ER). Tamoxifen (4-OHT) treatment induces DNA breakage in the Sμ and Sα regions but not in the Sγ region of JP8Bdel-ER-expressing CH12 cells, which switch almost exclusively from IgM to IgA (8).

BL2-ΔC-AIDER cells were treated with 4-OHT only for 3 h to minimize cell death and DNA break ends were labeled with a biotinylated linker, and the break-enriched biotinylated DNA was used as a PCR template (Fig. 1*A*). In agreement with previous reports (8, 42), we detected DNA breakage in the 5′ Sμ region of the IgH locus only in 4-OHT–treated cells. No breakage was detected in the *B2M* gene, which is expressed in BL2 cells but was shown not to accumulate mutations in activated B cells (Fig. 1*B*).

AID Targets Identified by Promoter Array and Whole Genome Sequencing. Because SHM is normally detected close to the TSS (13, 14), biotin linker-enriched DNA fragments were analyzed by a promoter array to identify unknown AID targets. Table S1 lists the genes whose signals increased after 3 h of 4-OHT treatment, compared with untreated samples with false discovery rate (FDR) values <0.3. We also looked for genes with increased signals after 4-OHT treatment that are known to be targets of chromosomal translocation or genes that had multiple breakage peaks, and we identified >50 genes, among which we found that *BCL7A* and *CUX1* are enriched in the original breakage-enriched library by qPCR (see below). We confirmed by RT-PCR and expression array that *SNHG3*, *MALAT1*, *NIN*, *C9orf72*, *CFLAR*, *SNX25*, *BCL7A,* and *CUX1* were transcribed in BL2 cells (Table S1). Fig. S1 shows the peak signals in a 10-kb segment surrounding the breakage area of *SNHG3, MALAT1, BCL7A,* and *CUX1*. We could not map the breakage in the Ig locus because of the absence of array probes in this region.

Because the promoter array does not detect DNA fragments outside of regions containing probes, we further analyzed the breakage-enriched DNA by direct sequencing of the biotin linker-enriched library. DNA breakage sites in both control and 4-OHT–treated libraries were identified by aligning sequenced tags to the genome, and significantly enriched regions were identified by comparing the local breakage density (*SI Materials and Methods*). Regions were identified in the genes listed in Table S2. Interestingly, *SNHG3* and *MALAT1*, which were identified by the promoter array, appear at the top of the list in the genome-wide sequencing as well.

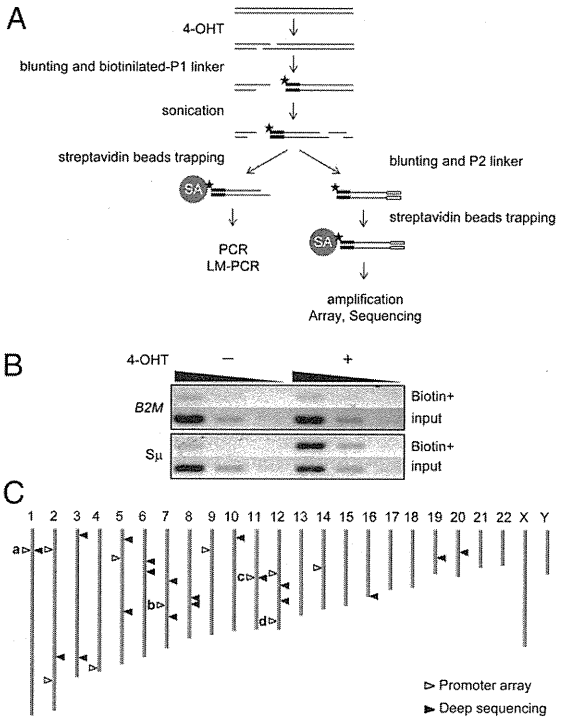

Fig. 1. (*A*) Schematic of the labeling technique. 4-OHT is added to activate AID, and DNA break ends are labeled in situ by biotinylated linker ligation. After genomic DNA is extracted and sonicated, biotinylated fragments are captured by streptavidin beads and used for PCR, array, or sequencing. (*B*) Detection of DNA breaks by PCR. BL2-ΔC-AIDER cells were treated with or without 4-OHT for 3 h, and the break ends were labeled. PCR of Sμ and *B2M* was performed with biotin-labeled DNA or input DNA by using fivefold serially diluted templates. (*C*) Chromosomal distribution of AID targets. a, *SNHG3*; b, *CUX1*; c, *MALAT1*; d, *BCL7A*. White arrowhead, promoter array (FDR < 0.3 plus *BCL7A* and *CUX1*); black arrowhead, whole genome sequencing (FDR < 0.01 and/or remarkable numbers of *P* value clusters).

Fig. 1*C* shows the chromosomal distribution of AID target candidates identified by promoter array or whole-genome sequencing. Breakage seemed to be distributed through the genome without any apparent bias. Surprisingly, of the 29 candidates identified by whole-genome sequencing with strict statistical parameters, only two matched candidates obtained from the promoter array. This discrepancy might be explained in part because most of the breakage-rich regions detected by whole genome sequencing are located in regions that do not contain promoter array probes.

Results may also be limited because of possible bias by PCR amplification of the primary library for microarray and whole-genome sequencing, which could affect the relative genome coverage. To avoid this bias, we relied on the original library and confirmed all candidates by qPCR.

qPCR Analyses of Linker Libraries. To confirm the AID-induced breakage candidates detected by the promoter array and whole-genome sequencing, we used qPCR assays with gene-specific primers to amplify the vicinity of the identified breakage regions in biotin linker-enriched DNA from cells treated with 4-OHT for 3 h (Fig. 2). We examined whether candidate genes were enriched in the 4-OHT–treated DNA library compared with the nontreated library. Among the 29 candidates identified by whole-genome sequencing, only *SNHG3* and *MALAT1* were strongly enriched ($P < 0.0001$ and $P < 0.001$, respectively). Besides these, *BCL7A*, *CUX1,* and *CFLAR*, which were picked up only by the

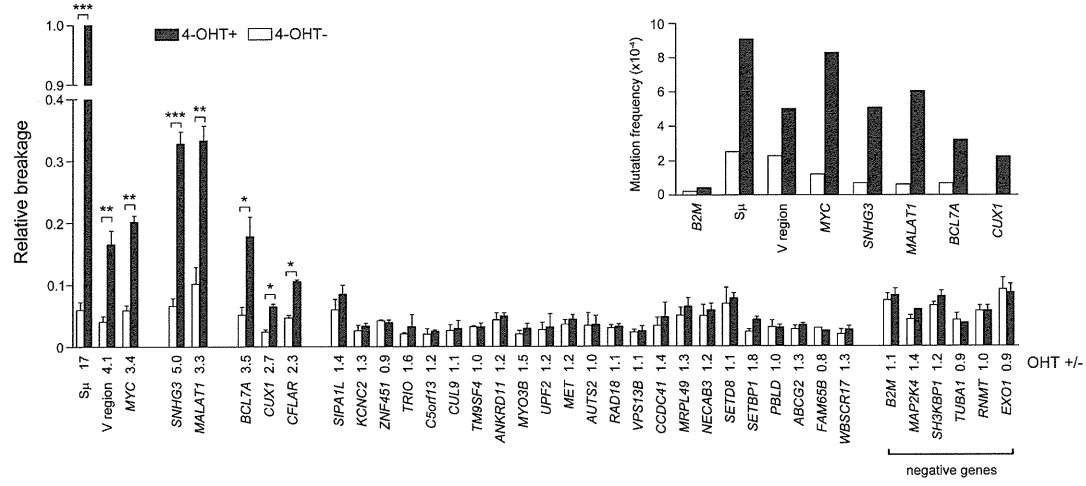

Fig. 2. qPCR measurement of DNA breaks. Break signals are presented relative to Sμ. SD values were derived from at least three independent experiments, and *P* values were calculated by a two-tailed *t* test. $*P < 0.01$, $**P < 0.001$, $***P < 0.0001$. Numbers below the *x* axis indicate the ratio between samples treated and not treated with 4-OHT. (*Inset*) Mutation analysis of genes with significantly increased break signals after AID activation. Cells were treated with or without 4-OHT for 24 h. Only unique mutations were counted. Detailed mutation profiles can be found in Fig. S2 and Table S3.

promoter array, also showed significant enrichment ($P < 0.01$) in the 4-OHT–treated library.

We also confirmed that the Sμ and V regions in BL2 cells were cleaved, because they were enriched in the 4-OHT–treated library. Although *MYC*, which is translocated in an AID-dependent manner in human Burkitt's lymphoma (44), was not identified by either promoter array or whole-genome sequencing, qPCR of the 4-OHT–treated samples clearly revealed *MYC* gene enrichment (Fig. 2). The difference in cleavage detection between the direct candidate qPCR and genome-wide arrays and sequencing suggests that the amplification step required for microarray and whole-genome sequencing methods may introduce bias, either for or against many genes. In the case of sequencing, this bias can lead to low mapping coverage of certain regions, hampering efforts to identify significant enrichment. Therefore, we cannot exclude genes that were not identified by the present methods from being AID targets.

AID Targets Accumulate Somatic Mutations near Cleavage Sites. To test whether the newly identified target genes are mutated upon AID activation, we treated BL2-ΔC-AIDER cells with 4-OHT for 24 h and sequenced regions of ≈600 bp around each area with abundant breakage (Fig. S2 and Table S3). Mutations increased in all of the qPCR-confirmed AID target genes after 4-OHT treatment (Fig. 2, *Inset*), with mutation frequencies ranging from 6.1×10^{-4} for *MALAT1* to 2.2×10^{-4} for *CUX*. These frequencies are comparable to those of the V region (5.0×10^{-4}), the Sμ region (9.1×10^{-4}), and the *MYC* gene (8.3×10^{-4}), and are far higher than that of the control *B2M* gene (4.3×10^{-5}). We also detected mutations in the *CFLAR* gene; however, the mutation frequency (9.2×10^{-5}) was not as high as other AID target genes, although mutations increased significantly in 4-OHT–treated sample ($P = 0.004$) (Table S3).

To compare the distribution profiles of mutated bases and AID-induced DNA breaks in the biotin linker-enriched DNA, we mapped the linker positions by performing ligation-mediated (LM)-PCR with the linker primer and gene-specific primers. These PCR fragments were subsequently cloned and sequenced. Break ends identified by the linker were plotted, together with mutation positions (Fig. 3 and Fig. S2). The results clearly showed that the DNA cleavage marks (biotin linker) were closely associated with mutations, indicating that the DNA cleavage sites identified are functionally relevant to SHM by AID. We used RT-PCR and expression arrays to confirm that the regions

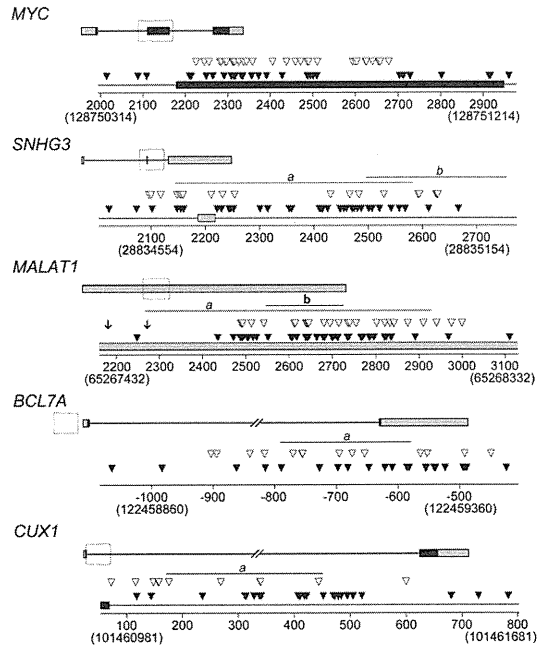

Fig. 3. Somatic mutations and breakpoint distribution in AID target loci. Mutations (open triangles) and breakpoints (filled triangles) detected by LM-PCR (Fig. S2) were plotted on the respective genomic sequences. The top scheme represents exons (rectangles) and introns (bars). Genomic loci are shown in untranslated and translated sequences (gray and black boxes, respectively). The horizontal lines *a* and *b* represent breakage regions identified by promoter array and sequencing, respectively. Regions outlined by dotted boxes are shown in more detail below each genomic locus. For the *MALAT1* locus, the translocation breakpoints reported by Davis et al. (45) are represented by arrows. *x* axis numbers indicate base positions according to RefSeq: NM_002467 (*MYC*), NR_002909 (*SNHG3*), NR_002819 (*MALAT1*), NM_020993 (*BCL7A*), and NM_181552 (*CUX1*). Numbers in parentheses indicate the corresponding base position according to hg19 assembly.

where DNA cleavage and mutations were identified are transcribed (Tables S1 and S2).

Repetitive Sequences Surround the Breakage Regions of Unique Targets. We next examined common features among the AID targets. Although SHM has been reported to prefer the RGYW-WRCY motif (46), we could not find any enrichment of this motif among the break sites in the newly identified targets. It was recently reported that mutations are introduced in regions with sequences prone to forming non-B DNA structure, including tandem repeats, palindromes, and inverted repeats (17, 18). The S region, *MYC,* and V region genes contain sequences prone to forming non-B structure (19, 20, 47, 48). We used REPFIND, a program that identifies clustered, nonrandom short repeats in a given nucleotide sequence, to search the vicinity of identified breakage regions for sequences prone to forming non-B structure. For each repeat cluster, a *P* value is calculated indicating the probability of finding such a repeat cluster randomly (a *P* value of 1×10^{-5} means that such a concentration of that particular repeat occurs an average of once in 100,000 bp by chance) (49). Curiously, we found that various types of repeat sequences cluster in the vicinity of cleaved sites in the newly identified AID target genes. In the *MALAT1* locus, the region within 2 kb surrounding the breakage peaks was rich in clustered short repeat motifs such as GAAG, GCC, GAA, CCG, AAG, GAAGA, and TTAA (Fig. 4). Repeat clusters were also found near the cleavage sites of the *SNHG3*, *BCL7A,* and *CUX1* loci. (Fig. S3). In all cases, the probability of the appearance of these repeats was far below random ($P < 1 \times 10^{-8}$).

H3K4me3 at Cleavage Sites. It was recently shown that S region transcription alone is not sufficient for CSR; specific histone posttranslational modification marks, especially H3K4me3, are required. H3K4me3 depletion strongly inhibits CSR and DNA cleavage in the Sμ and Sα regions (15). We thus asked whether the V region and the newly identified AID targets also carry H3K4me3 marks around the cleavage regions. ChIP analysis showed that both the V region and *MALAT1* locus were abundantly marked by H3K4me3 (Fig. 5). Furthermore, the H3K4me3 distribution profiles corresponded well to the somatic mutation distribution in the rearranged V region and to the breakage signal

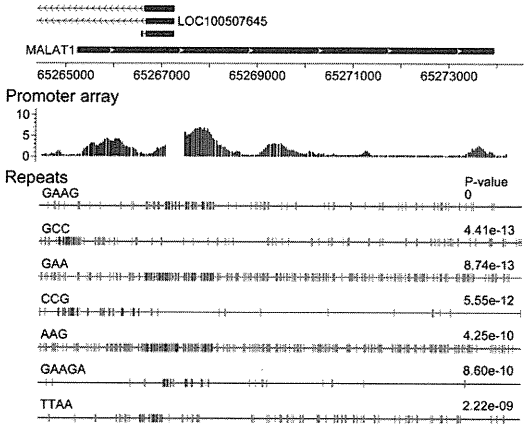

Fig. 4. Repeat sequences surrounding the breakage region in the *MALAT1* gene. (*Top*) Representation of a 10-kb segment surrounding the *MALAT1* locus. *x* axis numbers represent base positions according to hg19 assembly. (*Middle*) Breakage signal distribution detected by promoter array. Regions without bars do not have array probes. (*Bottom*) REPFIND analysis showing significant repeat clusters in the *MALAT1* locus. Motifs depicted as small, colored, vertical bars indicate the cluster with the most significant *P* value; individual repeats are separated by different colors.

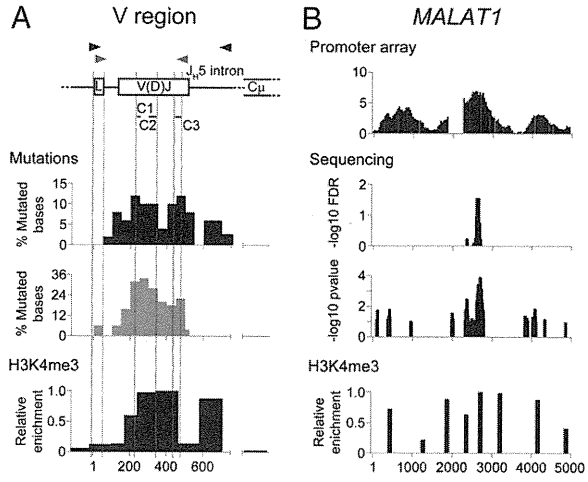

Fig. 5. H3K4me3 distribution in the IgH V region and in the *MALAT1* gene. (*A Top*: Representation of the rearranged IgH V region of BL2 cells. Black and gray arrowheads represent the position of primers used for the mutation analysis shown in *Bottom* (graphs in black and gray, respectively). L, leader; C1, CDR1; C2, CDR2; C3, CDR3. (*A Middle*) Somatic mutation distribution, represented as the percentage of mutated bases per 50 bp sequenced. Graph in black: mutations from Fig. 2, *Inset*. Graph in gray: mutations reported by Denepoux et al. (50). (*Bottom*) ChIP assay using an anti-H3K4me3 antibody. *x* axis numbers indicate the nucleotide position relative to the first V-gene ATG. (*B*) *MALAT1* locus. From top to bottom: Breakage signal distribution detected by promoter array (regions without bars do not have array probes); FDR regions by sequencing; *P* value peaks by sequencing; ChIP assay using an H3K4me3 antibody. *x* axis numbers indicate base positions according to RefSeq NR_002819.

distribution observed by both the promoter array and whole genome sequencing in *MALAT1* (Fig. 5 *A* and *B*). Mutations identified in *MALAT1* overlapped with DNA cleavage signals and H3K4me3 marks (Figs. 3 and 5*B*). We examined the H3K4me3 pattern of other AID targets by using publicly available ENCODE ChIP-seq data for the B-lymphoblastoid cell line GM12878 (51). As expected, all of them, except for *BCL7A*, were highly abundant in H3K4me3 marks overlapping nicely with cleavage sites (Fig. S4). H3K4me3 might be absent at the *BCL7A* locus in GM12878 cells because it is an inducible gene expressed in BL2 cells, but not in the GM12878 cell line (52). We thus conclude that the newly identified AID targets share both *cis* and *trans* marks for AID targeting—non-B structure and H3K4me3, respectively (15, 16).

Discussion

Identified AID Targets Accumulate High-Frequency Mutations. We explored AID targets by combining three different strategies: promoter array, whole genome sequencing, and candidate qPCR in a library containing biotinylated linker-labeled cleaved ends. With these strong criteria, we were able to identify four unique AID targets: *SNHG3, MALAT1, BCL7A,* and *CUX1*. All of these candidates were further confirmed to accumulate mutations. These candidates are thus strong AID cleavage targets; however, these genes represent only very efficient AID targets. The use of the biotinylated linker, which efficiently identifies double-strand breakage with close, staggered nicks on opposite strands, may not detect scattered nicks efficiently, and this may limit identification to targets that are efficiently and specifically cleaved within 3 h of AID activation.

Some well-described SHM target genes, including *MYC, BCL6, PAX5, RHOH,* and *PIM1,* were not detected by either the promoter array or whole genome sequencing. We used qPCR to test whether these genes were enriched in the biotin-labeled

DNA library, but only *MYC* was enriched in the 4-OHT–treated sample (Fig. 2). These genes have been found to be mutated in memory and GC B cells as well as lymphoma cells (24, 32, 36, 37), cells that are expected to be chronically exposed to AID. In addition, the mutation accumulation in tumor cells depends on selection. In contrast, in our study, we exposed BL2 cells to a short treatment (3 h) of 4-OHT, to increase the chance of detecting only efficiently targeted loci. In fact, none of the genes above mentioned mutated more than 1/20th of the 3′ J_H locus even in 6-mo-old Peyer's patch B cells (36).

The unique AID targets accumulate mutations at comparable frequencies with the *Ig* and *MYC* genes. We found that the mutation and cleavage sites are located in similar areas. The results indicate that the cleavage and mutation sites are linked, but not necessarily identical. This observation is consistent with the prediction that SHM is incorporated during the repair phase by error-prone polymerases (53). We confirmed that all of the newly identified AID targets were highly transcribed in BL2 cells. Although the breakage signal detected at the *BCL7A* locus was ≈800 bp upstream of the TSS, we detected both sense and antisense transcripts in this region.

Unique AID Targets also Translocate. Furthermore, it is important to stress that all of these unique candidates have been shown to be the targets of chromosomal translocation in neoplastic cells as shown for the *Ig* locus and *MYC* gene. MALAT1 is overexpressed in several cancers and was reported to be involved in regulating alternative splicing (54). The *MALAT1* locus has been found to harbor chromosomal translocation breakpoints associated with cancer (45, 55) and, interestingly, two reported translocation breakpoints are close to or within the breakage region identified in the present study (Fig. 3). *SNHG3*, a host gene for small nucleolar RNAs (56), is also reported to be involved in translocation, and although the exact position of the translocation breakpoint has not been reported, we can speculate that it is located in the second intron of *SNHG3* because the detected fusion transcript joins the second exon of *SNHG3* with the exon of the 3′ partner gene (57). *BCL7A* and *CUX1* have also been reported to bear chromosomal translocations; however, these translocation breakpoints occur far from the breakage regions identified in this study (58, 59).

Abundant Repetitive Sequences in AID Targets. To identify common features of AID targets, we compared the *MYC*, *SNHG3*, *MALAT1*, *CUX1*, and *BCL7A* genes with the Ig gene locus (the V_H gene and the Sμ region). Sequence analysis identified abundant repetitive sequences surrounding the cleaved regions of AID targets. A typical example is *MALAT1* (Fig. 4): The GAAG, GCC, GAA, CCG, AAG, GAAGA, and TTAA repeats are highly abundant within 2 kb surrounding the break peaks, which also overlap with actual mutation sites. In the *SNHG3* locus, less frequent but longer repeats—GGATTACAG, TTTTTGTATTTT, ATTACAGGC, GCCTC, and TTTTTGTA—are clustered in the proximity of cleavage sites (Fig. S3*A*). *BCL7A* and *CUX1* have GC-rich repeats, such as CGCG, CCGCG, CCCG, and CGGCG (Fig. S2 *B* and *C*). The *MYC* gene, the V region, and the S region are already known to have repetitive sequences or inverted repeats that can form non-B structure when the target is actively transcribed and under an excessive negative superhelical condition (19, 20, 47, 48).

H3K4me3 Marks in AID Targets. Chromatin modifications are also involved in AID targeting. We showed that H3K4 methylation, specifically trimethylation, is critical for DNA cleavage in the S region (15), although Odegard et al. (60) showed that the H3K4 dimethylation (H3K4me2) pattern is similar among VJλ1, Cλ1, and Eλ3-1 and concluded that H3K4me2 is not correlated with SHM. Association of H3K4me3 with the MYC locus was also reported (38). Therefore, we tested whether H3K4me3 modification is also associated with the V region and the unique loci. SHM in V regions typically targets the whole coding V-region segment and extends to its 5′ and 3′ flanking regions. Mutation frequencies rise sharply ≈100 bp downstream of the TSS (at the middle of the leader intron), peak in V(D)J, and then gradually decrease after the immediate 3′ flanking region, becoming undetectable over a distance of ≈1 kb from the rearranged J (61). It is striking that the H3K4me3 profile follows the exact same tendency as SHM distribution in the V region (Fig. 5*A*). H3K4me3 is scarce in the leader exon and intron but present in the highly mutated portion of the V(D)J exon. We also observed that H3K4me3 distribution at the *MALAT1* locus corresponded well with the breakage signal distribution detected by both the promoter array and whole genome sequencing (Fig. 5*B* and Fig. S3*A*). The H3K4me3 pattern of other AID targets also overlaps with cleavage sites (Fig. S3 *B–D*). Strikingly, we observed a strong H3K4me3 peak in the 5′ region of the *CUX1* gene (Fig. S4*D*), which does not contain microarray probes. We confirmed that this region also accumulates mutations after 4-OHT treatment (Table S3). It would be interesting to check whether H3K4me3 depletion can decrease AID-induced breaks and mutations in the newly identified AID targets.

We thus conclude that all of these genes, *SNHG3, MALAT1, BCL7A,* and *CUX1*, share unique characteristics that are required for AID targeting: non-B structure as the *cis* element and the H3K4me3 histone modification as the *trans* mark.

Materials and Methods

Labeling of DNA Break Ends by a Biotinylated Linker. The biotin-labeled DNA break assay was performed as described (8) with slight modifications. After nuclear permeabilization, BL2 cells were washed with cold PBS and resuspended in 1× T4 DNA polymerase buffer. Blunting was performed by using T4 DNA Polymerase (Takara). After washing with cold PBS, 4 μL of T4 DNA Ligase (Takara) and 13.4 μL of an annealed biotinylated P1 linker were added, and the cells were incubated overnight at 16 °C. Genomic DNA was purified by phenol:chloroform extraction.

PCR, Real-Time PCR, and LM-PCR. Biotinylated genomic DNA (10 μg) was sonicated (Covaris) and incubated with 10 μL of M-270 Dynabeads (Invitrogen) for 15 min at room temperature. After washing, the beads were resuspended in 15 μL of TE buffer and used as a PCR template. PCR was initiated by denaturing for 5 min at 95 °C followed by 25 cycles (95 °C for 30 s, 60 °C for 30 s, and 72 °C for 30 s) and a final extension at 72 °C for 5 min. SYBR Green Master Mix (Applied Biosystems) was used for real-time PCR.

For LM-PCR, we used a template of 1 μL of beads in a two-round PCR by using linker primer (P1-LM) and gene-specific primers. First-round PCR was initiated by nick translation (72 °C for 20 min), followed by denaturing (95 °C for 5 min), 25 cycles (95 °C for 15 s, 65 °C for 15 s, and 70 °C for 1 min), and a final extension (70 °C for 5 min). Second-round PCR included denaturing (95 °C for 5 min), 20 cycles (95 °C for 15 s, 65 °C for 15 s, and 70 °C for 1 min), and a final extension (70 °C for 7 min). The PCR fragments were purified, cloned with the pGEM-T Easy Vector System (Promega), and sequenced with the ABI PRISM 3130xl Genetic Analyzer (Applied Biosystems). Primers sequences are provided in Table S4–S7.

DNA Preparation for Microarray and SOLiD Sequencing. After sonication of biotin-labeled genomic DNA, sheared ends were blunted by adding T4 DNA polymerase for 30 min at room temperature. DNA was purified by using the PureLink PCR purification Kit (Invitrogen), P2-annealed linker was ligated overnight at 16 °C, DNA was incubated with Dynabeads as described above, and the beads were used for global amplification by following the SOLiD protocol (Applied Biosystems). A summary of general features of the sequenced libraries can be found in Fig. S5 and Table S8.

Accession Codes. Gene Expression Omnibus: microarray data, GSE32027; DNA Data Bank of Japan: sequencing data, DRA000450.

Other material and methods are provided in *SI Materials and Methods*.

ACKNOWLEDGMENTS. We thank Y. Shiraki for manuscript preparation, Dr. H. Nagaoka for sharing unpublished BL2 expression data, and RIKEN Genome Network Analysis Service (GeNAS) for library sequencing using the

SOLiD system (Life Technologies). This research was supported by a RIKEN Omics Science Center from the Ministry of Education, Culture, Sports, Science and Technology (MEXT) of Japan research grant (to Y.H.) and MEXT of Japan Grant-in-Aid for Specially Promoted Research 17002015.

1. Muramatsu M, et al. (2000) Class switch recombination and hypermutation require activation-induced cytidine deaminase (AID), a potential RNA editing enzyme. *Cell* 102:553–563.
2. Revy P, et al. (2000) Activation-induced cytidine deaminase (AID) deficiency causes the autosomal recessive form of the Hyper-IgM syndrome (HIGM2). *Cell* 102:565–575.
3. Honjo T, Kinoshita K, Muramatsu M (2002) Molecular mechanism of class switch recombination: Linkage with somatic hypermutation. *Annu Rev Immunol* 20:165–196.
4. Teng G, Papavasiliou FN (2007) Immunoglobulin somatic hypermutation. *Annu Rev Genet* 41:107–120.
5. Shinkura R, et al. (2004) Separate domains of AID are required for somatic hypermutation and class-switch recombination. *Nat Immunol* 5:707–712.
6. Barreto V, Reina-San-Martin B, Ramiro AR, McBride KM, Nussenzweig MC (2003) C-terminal deletion of AID uncouples class switch recombination from somatic hypermutation and gene conversion. *Mol Cell* 12:501–508.
7. Ta VT, et al. (2003) AID mutant analyses indicate requirement for class-switch-specific cofactors. *Nat Immunol* 4:843–848.
8. Doi T, et al. (2009) The C-terminal region of activation-induced cytidine deaminase is responsible for a recombination function other than DNA cleavage in class switch recombination. *Proc Natl Acad Sci USA* 106:2758–2763.
9. Jung S, Rajewsky K, Radbruch A (1993) Shutdown of class switch recombination by deletion of a switch region control element. *Science* 259:984–987.
10. Peters A, Storb U (1996) Somatic hypermutation of immunoglobulin genes is linked to transcription initiation. *Immunity* 4:57–65.
11. Betz AG, et al. (1994) Elements regulating somatic hypermutation of an immunoglobulin kappa gene: Critical role for the intron enhancer/matrix attachment region. *Cell* 77:239–248.
12. Zhang J, Bottaro A, Li S, Stewart V, Alt FW (1993) A selective defect in IgG2b switching as a result of targeted mutation of the I gamma 2b promoter and exon. *EMBO J* 12: 3529–3537.
13. Hackett J, Jr., Rogerson BJ, O'Brien RL, Storb U (1990) Analysis of somatic mutations in kappa transgenes. *J Exp Med* 172:131–137.
14. O'Brien RL, Brinster RL, Storb U (1987) Somatic hypermutation of an immunoglobulin transgene in kappa transgenic mice. *Nature* 326:405–409.
15. Stanlie A, Aida M, Muramatsu M, Honjo T, Begum NA (2010) Histone3 lysine4 trimethylation regulated by the facilitates chromatin transcription complex is critical for DNA cleavage in class switch recombination. *Proc Natl Acad Sci USA* 107:22190–22195.
16. Kobayashi M, et al. (2009) AID-induced decrease in topoisomerase 1 induces DNA structural alteration and DNA cleavage for class switch recombination. *Proc Natl Acad Sci USA* 106:22375–22380.
17. Hubert L, Jr., Lin Y, Dion V, Wilson JH (2011) Topoisomerase 1 and single-strand break repair modulate transcription-induced CAG repeat contraction in human cells. *Mol Cell Biol* 31:3105–3112.
18. Zhao J, Bacolla A, Wang G, Vasquez KM (2010) Non-B DNA structure-induced genetic instability and evolution. *Cell Mol Life Sci* 67:43–62.
19. Rogozin IB, Solovyov VV, Kolchanov NA (1991) Somatic hypermutagenesis in immunoglobulin genes. I. Correlation between somatic mutations and repeats. Somatic mutation properties and clonal selection. *Biochim Biophys Acta* 1089:175–182.
20. Wright BE, Schmidt KH, Minnick MF, Davis N (2008) I. VH gene transcription creates stabilized secondary structures for coordinated mutagenesis during somatic hypermutation. *Mol Immunol* 45:3589–3599.
21. Lippert MJ, et al. (2011) Role for topoisomerase 1 in transcription-associated mutagenesis in yeast. *Proc Natl Acad Sci USA* 108:698–703.
22. Takahashi T, Burguiere-Slezak G, Van der Kemp PA, Boiteux S (2011) Topoisomerase 1 provokes the formation of short deletions in repeated sequences upon high transcription in Saccharomyces cerevisiae. *Proc Natl Acad Sci USA* 108:692–697.
23. Okazaki IM, et al. (2003) Constitutive expression of AID leads to tumorigenesis. *J Exp Med* 197:1173–1181.
24. Kotani A, et al. (2005) A target selection of somatic hypermutations is regulated similarly between T and B cells upon activation-induced cytidine deaminase expression. *Proc Natl Acad Sci USA* 102:4506–4511.
25. Ramiro AR, et al. (2004) AID is required for c-myc/IgH chromosome translocations in vivo. *Cell* 118:431–438.
26. Takizawa M, et al. (2008) AID expression levels determine the extent of cMyc oncogenic translocations and the incidence of B cell tumor development. *J Exp Med* 205: 1949–1957.
27. Ishikawa C, Nakachi S, Senba M, Sugai M, Mori N (2011) Activation of AID by human T-cell leukemia virus Tax oncoprotein and the possible role of its constitutive expression in ATL genesis. *Carcinogenesis* 32:110–119.
28. Machida K, et al. (2004) Hepatitis C virus induces a mutator phenotype: Enhanced mutations of immunoglobulin and protooncogenes. *Proc Natl Acad Sci USA* 101: 4262–4267.
29. Epeldegui M, Hung YP, McQuay A, Ambinder RF, Martínez-Maza O (2007) Infection of human B cells with Epstein-Barr virus results in the expression of somatic hypermutation-inducing molecules and in the accrual of oncogene mutations. *Mol Immunol* 44:934–942.
30. Matsumoto Y, et al. (2007) Helicobacter pylori infection triggers aberrant expression of activation-induced cytidine deaminase in gastric epithelium. *Nat Med* 13:470–476.
31. Faili A, et al. (2002) AID-dependent somatic hypermutation occurs as a DNA single-strand event in the BL2 cell line. *Nat Immunol* 3:815–821.
32. Pasqualucci L, et al. (2001) Hypermutation of multiple proto-oncogenes in B-cell diffuse large-cell lymphomas. *Nature* 412:341–346.
33. Pasqualucci L, et al. (2004) Expression of the AID protein in normal and neoplastic B cells. *Blood* 104:3318–3325.
34. Feldhahn N, et al. (2007) Activation-induced cytidine deaminase acts as a mutator in BCR-ABL1-transformed acute lymphoblastic leukemia cells. *J Exp Med* 204:1157–1166.
35. Leuenberger M, et al. (2010) AID protein expression in chronic lymphocytic leukemia/small lymphocytic lymphoma is associated with poor prognosis and complex genetic alterations. *Mod Pathol* 23:177–186.
36. Liu M, et al. (2008) Two levels of protection for the B cell genome during somatic hypermutation. *Nature* 451:841–845.
37. Shen HM, Peters A, Baron B, Zhu X, Storb U (1998) Mutation of BCL-6 gene in normal B cells by the process of somatic hypermutation of Ig genes. *Science* 280:1750–1752.
38. Yamane A, et al. (2011) Deep-sequencing identification of the genomic targets of the cytidine deaminase AID and its cofactor RPA in B lymphocytes. *Nat Immunol* 12:62–69.
39. Staszewski O, et al. (2011) Activation-induced cytidine deaminase induces reproducible DNA breaks at many non-Ig Loci in activated B cells. *Mol Cell* 41:232–242.
40. Pavri R, et al. (2010) Activation-induced cytidine deaminase targets DNA at sites of RNA polymerase II stalling by interaction with Spt5. *Cell* 143:122–133.
41. Ju BG, et al. (2006) A topoisomerase IIbeta-mediated dsDNA break required for regulated transcription. *Science* 312:1798–1802.
42. Nagaoka H, Ito S, Muramatsu M, Nakata M, Honjo T (2005) DNA cleavage in immunoglobulin somatic hypermutation depends on de novo protein synthesis but not on uracil DNA glycosylase. *Proc Natl Acad Sci USA* 102:2022–2027.
43. Woo CJ, Martin A, Scharff MD (2003) Induction of somatic hypermutation is associated with modifications in immunoglobulin variable region chromatin. *Immunity* 19: 479–489.
44. Dalla-Favera R, et al. (1982) Human c-myc onc gene is located on the region of chromosome 8 that is translocated in Burkitt lymphoma cells. *Proc Natl Acad Sci USA* 79:7824–7827.
45. Davis IJ, et al. (2003) Cloning of an Alpha-TFEB fusion in renal tumors harboring the t(6;11)(p21;q13) chromosome translocation. *Proc Natl Acad Sci USA* 100:6051–6056.
46. Rogozin IB, Kolchanov NA (1992) Somatic hypermutagenesis in immunoglobulin genes. II. Influence of neighbouring base sequences on mutagenesis. *Biochim Biophys Acta* 1171:11–18.
47. Tashiro J, Kinoshita K, Honjo T (2001) Palindromic but not G-rich sequences are targets of class switch recombination. *Int Immunol* 13:495–505.
48. Michelotti GA, et al. (1996) Multiple single-stranded cis elements are associated with activated chromatin of the human c-myc gene in vivo. *Mol Cell Biol* 16:2656–2669.
49. Betley JN, Frith MC, Graber JH, Choo S, Deshler JO (2002) A ubiquitous and conserved signal for RNA localization in chordates. *Curr Biol* 12:1756–1761.
50. Denépoux S, et al. (1997) Induction of somatic mutation in a human B cell line in vitro. *Immunity* 6:35–46.
51. Birney E, et al.; ENCODE Project Consortium; NISC Comparative Sequencing Program; Baylor College of Medicine Human Genome Sequencing Center; Washington University Genome Sequencing Center; Broad Institute; Children's Hospital Oakland Research Institute (2007) Identification and analysis of functional elements in 1% of the human genome by the ENCODE pilot project. *Nature* 447:799–816.
52. Ernst J, et al. (2011) Mapping and analysis of chromatin state dynamics in nine human cell types. *Nature* 473:43–49.
53. Faili A, et al. (2004) DNA polymerase eta is involved in hypermutation occurring during immunoglobulin class switch recombination. *J Exp Med* 199:265–270.
54. Tripathi V, et al. (2010) The nuclear-retained noncoding RNA MALAT1 regulates alternative splicing by modulating SR splicing factor phosphorylation. *Mol Cell* 39: 925–938.
55. Rajaram V, Knezevich S, Bove KE, Perry A, Pfeifer JD (2007) DNA sequence of the translocation breakpoints in undifferentiated embryonal sarcoma arising in mesenchymal hamartoma of the liver harboring the t(11;19)(q11;q13.4) translocation. *Genes Chromosomes Cancer* 46:508–513.
56. Pelczar P, Filipowicz W (1998) The host gene for intronic U17 small nucleolar RNAs in mammals has no protein-coding potential and is a member of the 5'-terminal oligopyrimidine gene family. *Mol Cell Biol* 18:4509–4518.
57. Levin JZ, et al. (2009) Targeted next-generation sequencing of a cancer transcriptome enhances detection of sequence variants and novel fusion transcripts. *Genome Biol* 10:R115.
58. Zani VJ, et al. (1996) Molecular cloning of complex chromosomal translocation t(8;14;12)(q24.1;q32.3;q24.1) in a Burkitt lymphoma cell line defines a new gene (BCL7A) with homology to caldesmon. *Blood* 87:3124–3134.
59. Wasag B, Lierman E, Meeus P, Cools J, Vandenberghe P (2011) The kinase inhibitor TKI258 is active against the novel CUX1-FGFR1 fusion detected in a patient with T-lymphoblastic leukemia/lymphoma and t(7;8)(q22;p11). *Haematologica* 96:922–926.
60. Odegard VH, Kim ST, Anderson SM, Shlomchik MJ, Schatz DG (2005) Histone modifications associated with somatic hypermutation. *Immunity* 23:101–110.
61. Lebecque SG, Gearhart PJ (1990) Boundaries of somatic mutation in rearranged immunoglobulin genes: 5' boundary is near the promoter, and 3' boundary is approximately 1 kb from V(D)J gene. *J Exp Med* 172:1717–1727.

nature genetics

LETTERS

Meta-analysis identifies nine new loci associated with rheumatoid arthritis in the Japanese population

Yukinori Okada[1–3,40], Chikashi Terao[4,5,40], Katsunori Ikari[6,40], Yuta Kochi[1,2,40], Koichiro Ohmura[5], Akari Suzuki[1], Takahisa Kawaguchi[4], Eli A Stahl[7,8], Fina A S Kurreeman[7–9], Nao Nishida[10], Hiroko Ohmiya[3], Keiko Myouzen[1], Meiko Takahashi[4], Tetsuji Sawada[11], Yuichi Nishioka[12], Masao Yukioka[13], Tsukasa Matsubara[14], Shigeyuki Wakitani[15], Ryota Teshima[16], Shigeto Tohma[17], Kiyoshi Takasugi[18], Kota Shimada[17], Akira Murasawa[19], Shigeru Honjo[20], Keitaro Matsuo[21], Hideo Tanaka[21], Kazuo Tajima[22], Taku Suzuki[6,23], Takuji Iwamoto[6,23], Yoshiya Kawamura[24], Hisashi Tanii[25], Yuji Okazaki[26], Tsukasa Sasaki[27], Peter K Gregersen[28], Leonid Padyukov[29], Jane Worthington[30], Katherine A Siminovitch[31], Mark Lathrop[32,33], Atsuo Taniguchi[6], Atsushi Takahashi[3], Katsushi Tokunaga[10], Michiaki Kubo[34], Yusuke Nakamura[35], Naoyuki Kamatani[36], Tsuneyo Mimori[5], Robert M Plenge[7,8], Hisashi Yamanaka[6], Shigeki Momohara[6,41], Ryo Yamada[37,41], Fumihiko Matsuda[4,38,39,41] & Kazuhiko Yamamoto[1,2,41]

Rheumatoid arthritis is a common autoimmune disease characterized by chronic inflammation. We report a meta-analysis of genome-wide association studies (GWAS) in a Japanese population including 4,074 individuals with rheumatoid arthritis (cases) and 16,891 controls, followed by a replication in 5,277 rheumatoid arthritis cases and 21,684 controls. Our study identified nine loci newly associated with rheumatoid arthritis at a threshold of $P < 5.0 \times 10^{-8}$, including *B3GNT2, ANXA3, CSF2, CD83, NFKBIE, ARID5B, PDE2A-ARAP1, PLD4* and *PTPN2*. *ANXA3* was also associated with susceptibility to systemic lupus erythematosus ($P = 0.0040$), and *B3GNT2* and *ARID5B* were associated with Graves' disease ($P = 3.5 \times 10^{-4}$ and 2.9×10^{-4}, respectively). We conducted a multi-ancestry comparative analysis with a previous meta-analysis in individuals of European descent (5,539 rheumatoid arthritis cases and 20,169 controls). This provided evidence of shared genetic risks of rheumatoid arthritis between the populations.

Rheumatoid arthritis is a complex autoimmune disease characterized by inflammation and the destruction of synovial joints and affects up to 1% of the population worldwide. To date, more than 35 rheumatoid arthritis susceptibility loci, including *HLA-DRB1*, *PTPN22*, *PADI4*, *STAT4*, *TNFAIP3* and *CCR6*, among others, have been identified by GWAS in multiple populations[1–12] and by several meta-analyses of the original GWAS[13–16]. In particular, each meta-analysis of these GWAS uncovered a number of loci that were not identified in the single GWAS, leading to recognition of the enormous power of the meta-analysis approach for detecting causal genes in disease. However, these previous meta-analyses have been performed solely in European populations[13–16] and not in Asian ones. As multi-ancestry studies on validated rheumatoid arthritis susceptibility loci showed the existence of both population-specific and shared genetic components of rheumatoid arthritis[10,17], additional studies in Asian populations might provide useful insight into the underlying genetic architecture of rheumatoid arthritis, which would otherwise be difficult to capture using the studies in a single population. Here, we report a meta-analysis of GWAS and a replication study for rheumatoid arthritis in a Japanese population that was conducted by the Genetics and Allied research in Rheumatic diseases NETworking (GARNET) consortium[10,12]. We subsequently performed a multi-ancestry comparative analysis that incorporated results from a previously conducted meta-analysis of individuals of European ancestry[15].

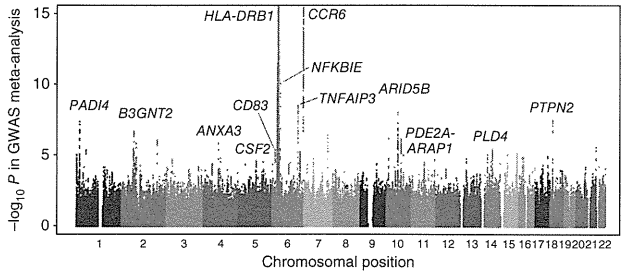

Figure 1 Manhattan plots of the GWAS meta-analysis for rheumatoid arthritis in the Japanese population. The genetic loci that satisfied the genome-wide significance threshold of $P < 5.0 \times 10^{-8}$ (gray line) in the meta-analysis or in the combined study of the meta-analysis and the replication study are presented. The *y* axis shows the $-\log_{10} P$ values of the SNPs in the meta-analysis. The SNPs for which the *P* values were smaller than 1.0×10^{-15} are indicated at the upper limit of the plot.

A full list of author affiliations appears at the end of the paper.

Received 24 October 2011; accepted 1 March 2012; published online 25 March 2012; doi:10.1038/ng.2231

Table 1 Results of the GWAS meta-analysis and the replication studies for rheumatoid arthritis

					Associations in Japanese							Associations in Europeans[c]			
					GWAS meta-analysis			Replication study		Combined study		GWAS meta-analysis			
					Allele 1 freq.							Allele 1 Freq.			
rsID[a]	Chr.	Position (bp)	Cytoband	Gene(s)	Allele 1/2	RA	Control	OR (95% CI)[b]	*P*	OR (95% CI)[b]	*P*	OR (95% CI)[b]	*P*	RA	Control	OR (95% CI)[b]	*P*
SNPs with significant associations ($P < 5.0 \times 10^{-8}$ in the combined study)																	
rs11900673	2	62306165	2p15	*B3GNT2*	T/C	0.31	0.28	1.15 (1.08–1.21)	3.5×10^{-6}	1.09 (1.04–1.14)	6.0×10^{-4}	1.11 (1.07–1.15)	1.1×10^{-8}	0.13	0.13	1.05 (0.98–1.13)	0.17
rs2867461	4	79732239	4q21	*ANXA3*	A/G	0.46	0.44	1.13 (1.08–1.19)	4.7×10^{-6}	1.12 (1.08–1.17)	1.2×10^{-7}	1.13 (1.09–1.17)	1.2×10^{-12}	0.37	0.37	0.98 (0.92–1.04)	0.52
rs657075	5	131458017	5q31	*CSF2*	A/G	0.38	0.36	1.12 (1.06–1.18)	3.2×10^{-5}	1.11 (1.06–1.16)	3.8×10^{-6}	1.12 (1.08–1.15)	2.8×10^{-10}	0.10	0.10	1.04 (0.95–1.13)	0.37
rs12529514	6	14204637	6p23	*CD83*	C/T	0.16	0.14	1.19 (1.10–1.27)	6.8×10^{-6}	1.11 (1.05–1.18)	6.0×10^{-4}	1.14 (1.09–1.19)	2.0×10^{-8}	0.055	0.053	1.11 (0.99–1.24)	0.074
rs2233434	6	44340898	6p21.1	*NFKBIE*	G/A	0.24	0.21	1.23 (1.16–1.31)	9.2×10^{-11}	1.17 (1.11–1.23)	2.2×10^{-9}	1.19 (1.15–1.24)	5.8×10^{-19}	0.059	0.040	1.57 (1.11–2.21)	0.0099
rs10821944	10	63455095	10q21	*ARID5B*	G/T	0.39	0.36	1.17 (1.11–1.23)	1.0×10^{-8}	1.15 (1.10–1.20)	3.0×10^{-10}	1.16 (1.12–1.20)	5.5×10^{-18}	0.29	0.26	1.11 (1.05–1.17)	1.9×10^{-4}
rs3781913	11	72051144	11q13	*PDE2A-ARAP1*	T/G	0.71	0.69	1.11 (1.05–1.17)	3.2×10^{-4}	1.13 (1.08–1.18)	6.7×10^{-7}	1.12 (1.08–1.16)	5.8×10^{-10}	0.45	0.43	1.04 (0.99–1.09)	0.13
rs2841277	14	104462050	14q32	*PLD4*	T/C	0.72	0.69	1.11 (1.05–1.18)	2.8×10^{-4}	1.18 (1.13–1.24)	7.0×10^{-12}	1.15 (1.11–1.19)	1.9×10^{-14}	0.47	0.46	1.02 (0.96–1.09)	0.54
rs2847297	18	12787694	18p11	*PTPN2*	G/A	0.37	0.33	1.16 (1.11–1.23)	3.5×10^{-8}	1.06 (1.01–1.11)	0.013	1.10 (1.07–1.14)	2.2×10^{-8}	0.36	0.34	1.10 (1.05–1.15)	9.2×10^{-5}
SNPs with suggestive associations ($5.0 \times 10^{-8} \leq P < 5.0 \times 10^{-6}$ in the combined study)																	
rs4937362	11	127997949	11q24	*ETS1-FLI1*	T/C	0.71	0.68	1.13 (1.07–1.19)	2.0×10^{-5}	1.07 (1.02–1.12)	0.0061	1.09 (1.06–1.13)	7.5×10^{-7}	0.46	0.44	1.06 (1.01–1.11)	0.015
rs3783637	14	54417868	14q22	*GCH1*	C/T	0.76	0.74	1.13 (1.07–1.20)	6.5×10^{-5}	1.07 (1.02–1.13)	0.0062	1.10 (1.06–1.14)	2.0×10^{-6}	0.88	0.88	0.99 (0.88–1.11)	0.87
rs1957895	14	60978085	14q23	*PRKCH*	G/T	0.40	0.39	1.12 (1.06–1.18)	4.1×10^{-5}	1.07 (1.02–1.12)	0.0022	1.09 (1.05–1.13)	3.6×10^{-7}	0.093	0.089	1.01 (0.95–1.07)	0.73
rs6496667	15	88694672	15q26	*ZNF774*	A/C	0.38	0.35	1.13 (1.07–1.19)	4.7×10^{-5}	1.07 (1.02–1.11)	0.0050	1.09 (1.05–1.13)	1.4×10^{-6}	0.21	0.20	1.07 (1.01–1.13)	0.031
rs7404928	16	23796341	16p12	*PRKCB1*	T/C	0.65	0.62	1.13 (1.07–1.19)	1.5×10^{-5}	1.05 (1.01–1.10)	0.026	1.08 (1.05–1.12)	4.0×10^{-6}	0.75	0.75	1.01 (0.94–1.09)	0.79
rs2280381	16	84576134	16q24	*IRF8*	T/C	0.86	0.84	1.16 (1.08–1.25)	1.0×10^{-4}	1.09 (1.03–1.15)	0.0049	1.12 (1.07–1.17)	2.4×10^{-6}	0.62	0.60	1.05 (0.99–1.11)	0.081
SNPs in previously reported rheumatoid arthritis susceptibility loci ($P < 5.0 \times 10^{-8}$ in the GWAS)																	
rs766449	1	17547439	1p36	*PADI4*	T/C	0.44	0.40	1.17 (1.11–1.24)	4.6×10^{-8}	–	–	–	–	0.38	0.37	1.09 (1.03–1.05)	0.0022
rs2157337	6	32609122	6p21.3	*HLA-DRB1*	C/T	0.59	0.44	1.99 (1.88–2.11)	2.6×10^{-118}	–	–	–	–	0.69	0.46	2.50 (2.39–2.62)	$< 1.0 \times 10^{-300}$
rs6932056	6	138284130	6q23	*TNFAIP3*	C/T	0.092	0.073	1.35 (1.23–1.49)	3.2×10^{-9}	–	–	–	–	0.044	0.034	1.41 (1.24–1.60)	1.3×10^{-7}
rs1571878	6	167460832	6q27	*CCR6*	C/T	0.54	0.48	1.31 (1.24–1.39)	3.2×10^{-19}	–	–	–	–	0.47	0.43	1.13 (1.08–1.19)	5.9×10^{-7}

Chr., chromosome; Freq., frequency; RA, rheumatoid arthritis; OR, odds ratio; CI, confidence interval.
[a]SNPs with $P < 5.0 \times 10^{-6}$ in the combined study of the GWAS meta-analysis and the replication study or SNPs with $P < 5.0 \times 10^{-8}$ in the GWAS meta-analysis are annotated according to forward strand and NCBI Build 36.3. Full results of the replication study are provided in **Supplementary Table 3**. [b]Odds ratio of allele 1. [c]Associations in the previous meta-analysis in European populations[15].

The meta-analysis included 4,074 rheumatoid arthritis cases (with 81.4% and 80.4% of the subjects being positive for antibody to cyclic citrullinated peptide (anti-CCP) and rheumatoid factor, respectively) and 16,891 controls from three GWAS of Japanese subjects (from the BioBank Japan Project[10,18], Kyoto University[12] and the Institute of Rheumatology Rheumatoid Arthritis (IORRA)[19]; **Supplementary Table 1**). After the application of stringent quality control criteria, including principal-component analysis (PCA; **Supplementary Fig. 1**) for each GWAS, the meta-analysis was conducted by evaluating ~2.0 million autosomal SNPs with minor allele frequencies (MAFs) ≥0.01, which were obtained through whole-genome imputation of genotypes on the basis of the HapMap Phase 2 East Asian panels (Japanese in Tokyo (JPT) and Han Chinese in Beijing (CHB)). The inflation factor of the test statistics in the meta-analysis λ_{GC} was as low as 1.036, suggesting no substantial effects of population structure (**Supplementary Table 2**). The quantile-quantile plot of *P* values showed a marked discrepancy in the values in its tail from those anticipated under the null hypothesis that there is no association—even after removal of the SNPs located in the human leukocyte antigen (HLA) region, the major rheumatoid arthritis susceptibility locus—thereby showing the presence of significant associations in the meta-analysis (**Supplementary Fig. 2**).

We identified seven loci in the current meta-analysis that satisfied the genome-wide significance threshold of $P < 5.0 \times 10^{-8}$. These included previously known rheumatoid arthritis susceptibility loci, such as *PADI4* at 1p36, *HLA-DRB1* at 6p21.3, *TNFAIP3* at 6q23 and *CCR6* at 6q27 (refs. 1,3,6,10,15) (the smallest $P = 2.6 \times 10^{-118}$ was found at the *HLA-DRB1* locus; **Fig. 1** and **Table 1**). To our knowledge, the other three loci identified, *NFKBIE* at 6p21.1, *ARID5B* at 10q21 and *PTPN2* at 18p11, are newly associated ($P = 9.2 \times 10^{-11}$, 1.0×10^{-8} and 3.5×10^{-8}, respectively).

To validate the associations identified in the meta-analysis, we conducted a replication study of two independent Japanese rheumatoid arthritis case-control cohorts (cohort 1: 3,830 rheumatoid arthritis cases and 17,920 controls, cohort 2: 1,447 rheumatoid arthritis cases and 3,764 controls; **Supplementary Table 1**). To increase the number of subjects and enhance statistical power, genotype data obtained from other GWAS projects conducted for non-autoimmune diseases in Japanese using Illumina platforms were used for the replication control panels. For each of the 46 loci that exhibited $P < 5.0 \times 10^{-4}$ in

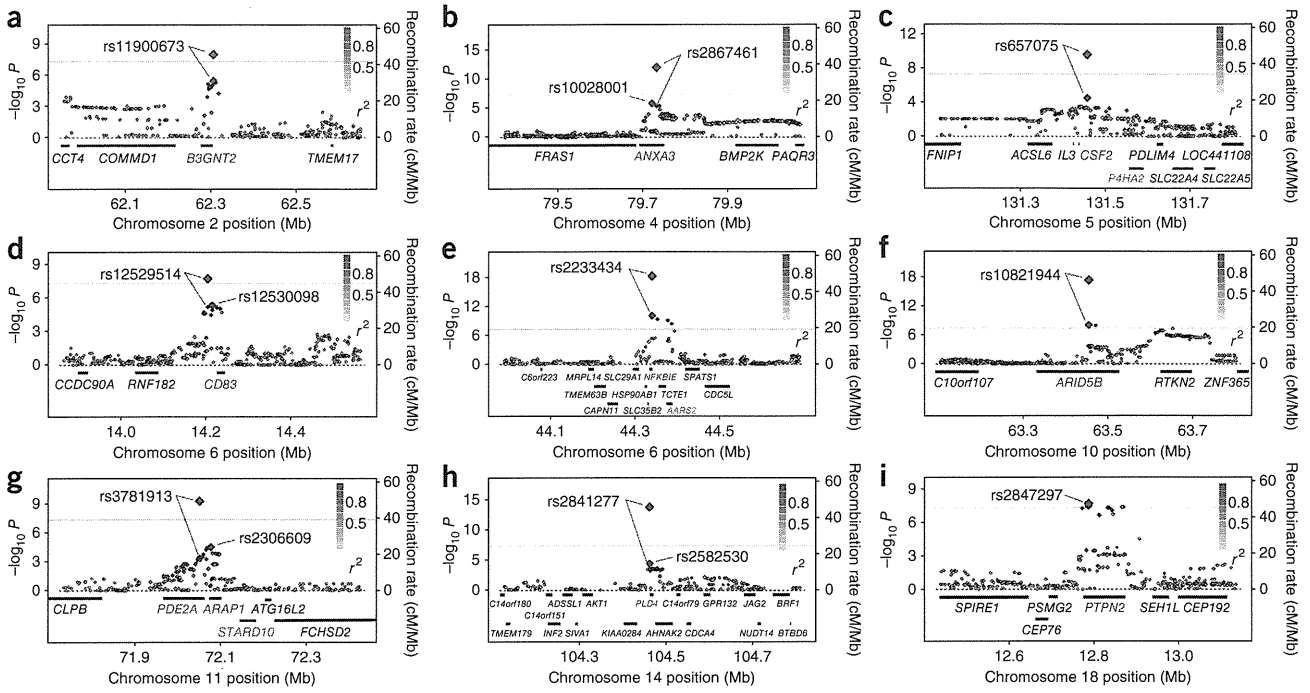

Figure 2 Regional plots of the loci newly associated with rheumatoid arthritis at the genome-wide significance threshold of $P < 5.0 \times 10^{-8}$ in the combined study of the meta-analysis and the replication study. (**a–i**) Regional plots are shown at *B3GNT2* (**a**), *ANXA3* (**b**), *CSF2* (**c**), *CD83* (**d**), *NFKBIE* (**e**), *ARID5B* (**f**), *PDE2A-ARAP1* (**g**), *PLD4* (**h**) and *PTPN2* (**i**). Diamonds represent the $-\log_{10} P$ values of the SNPs, and the red diamonds represent the $-\log_{10} P$ values of the SNPs in the meta-analysis. Red color for the smaller circles represents the r^2 value with the most significantly associated SNP (larger red circle). The purple circle represents the *P* value in the combined study. The blue line shows the recombination rates given by the HapMap Phase 2 east Asian populations (release 22). RefSeq genes at the loci are indicated below. Genes nearest to the marker SNPs at the loci are colored blue (**Supplementary Note**), and genes implicated in eQTL analysis are colored red (**Supplementary Table 4**). At 11q13, two genes (*PDE2A* and *ARAP1*) that are nearest to the SNP selected for the replication study and the most significant SNP in the meta-analysis are highlighted. The plots were drawn using SNP Annotation and Proxy Search (SNAP) version 2.2.

the meta-analysis and had not been reported as rheumatoid arthritis susceptibility loci[1–16], we selected a marker SNP for the replication study (Online Methods and **Supplementary Table 3**).

In the combined analyses of the meta-analysis and the replication study, including a total of 9,351 rheumatoid arthritis cases and 38,575 controls, we identified six newly associated loci, in addition to the *NFKBIE*, *ARID5B* and *PTPN2* loci, that satisfied the significance threshold of $P < 5.0 \times 10^{-8}$, including *B3GNT2* at 2p15, *ANXA3* at 4q21, *CSF2* at 5q31, *CD83* at 6p23, *PDE2A-ARAP1* at 11q13 and *PLD4* at 14q32 (**Figs. 1** and **2** and **Table 1**). Of these loci, *NFKBIE* had the smallest *P* value (5.8×10^{-19}). Although association with rheumatoid arthritis has been described for the *CSF2* and *PTPN2* loci[11,15,16,20,21], ours is the first report to our knowledge validating these associations with a threshold of $P < 5.0 \times 10^{-8}$. Suggestive associations were also observed in *ETS1-FLI1* at 11q24, *GCH1* at 14q22, *PRKCH* at 14q23, *ZNF774* at 15q26, *PRKCB1* at 16p12 and *IRF8* at 16q24 ($5.0 \times 10^{-8} \leq P < 5.0 \times 10^{-6}$). A summary of the genes in the newly associated loci and the results of *cis* expression quantitative trait locus (*cis* eQTL) analysis of the marker SNPs are provided (**Supplementary Table 4** and **Supplementary Note**).

Previous studies have reported associations of rheumatoid arthritis susceptibility loci with other autoimmune diseases[4,10,15,16]. Therefore, we assessed the association of these newly identified susceptibility loci with systemic lupus erythematosus (SLE) by examining the results of an SLE GWAS in the Japanese population (891 cases and 3,384 controls)[22] and in Graves' disease by genotyping 1,783 cases[10] (the controls from the SLE analysis were used for testing for Graves' disease). We observed significant associations of the *ANXA3* locus with SLE and of the *B3GNT2* and *ARID5B* loci with Graves' disease, which showed the same directional effects of the alleles as in rheumatoid arthritis ($P < 0.05/9 = 0.0056$, Bonferroni correction of the number of loci; **Supplementary Table 5**). It should be noted that relatively small sample sizes in the SLE and Graves' disease cohorts might yield limited statistical power, and further evaluations enrolling larger numbers of subjects would be desirable.

To highlight genetic backgrounds of rheumatoid arthritis that are common and divergent in different ancestry groups, we conducted a multi-ancestry comparative analysis of the present study in Japanese and a previous GWAS meta-analysis in Europeans that included 5,539 rheumatoid arthritis cases and 20,169 controls[15] (**Fig. 3a–c**). First, we compared associations in the reported[1–16] or newly identified rheumatoid arthritis susceptibility loci (**Fig. 3a** and **Supplementary Table 6**). Of the 46 rheumatoid arthritis risk variants evaluated, 6 were monomorphic in Japanese, and all were polymorphic in Europeans. We observed significant associations at 22 loci in Japanese and at 36 loci in Europeans (false discovery rate (FDR) < 0.05, $P < 0.0030$), with 14 loci being shared between the populations. Of the newly associated rheumatoid arthritis susceptibility loci identified in our Japanese meta-analysis, significant associations were also observed in the European meta-analysis at the *ARID5B* and *PTPN2* loci ($P = 1.9 \times 10^{-4}$ and 9.2×10^{-5}, respectively; **Table 1**). Significant positive correlation of odds ratios was observed between the studies ($r = 0.822$, $P = 8.1 \times 10^{-11}$; **Fig. 3b**), suggesting that a substantial proportion of genetic factors are shared between

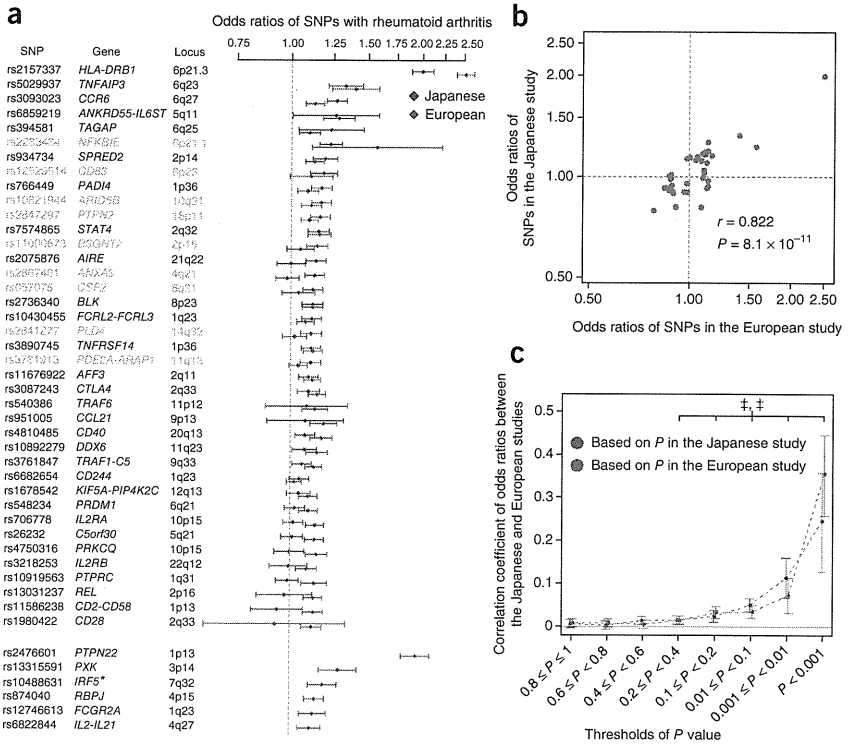

Figure 3 Overlap of the associations with rheumatoid arthritis between Japanese and European populations. (**a**) Forest plots of SNPs in the rheumatoid arthritis susceptibility loci (**Supplementary Table 6**). We selected the genetic loci that have been validated to be associated with rheumatoid arthritis susceptibility by showing associations in the reports of multiple cohorts or satisfying the genome-wide significant threshold ($P < 5.0 \times 10^{-8}$) in previous studies, including in the meta-analysis and replication phases[1–16]. For each of the loci, the most significant SNP among those reported in the previous or present study were selected[1–16]. SNPs in the newly identified rheumatoid arthritis susceptibility loci are colored green. Odds ratios and 95% confidence interval (CI) values are based on rheumatoid arthritis risk alleles, and the SNPs are ordered according to the odds ratios in the Japanese study. Several SNPs were monomorphic in the Japanese population. The odds ratios of these SNPs in the European study are presented below. The asterisk indicates that an association of another variant at the *IRF5* locus was reported in the Japanese population[24]. (**b**) Correlation of the odds ratios of the SNPs in the validated rheumatoid arthritis susceptibility loci between the two populations. SNPs that were polymorphic in both populations were used; odds ratios were based on the minor allele in the Japanese population. (**c**) Correlation of the odds ratios of the genome-wide SNPs, excluding the rheumatoid arthritis susceptibility loci. Correlations were evaluated for sets of SNPs stratified by the thresholds based on the meta-analysis *P* values in each population after pruning of the SNPs by LD ($r^2 < 0.3$). Correlation coefficient and 95% CI are indicated on the *y* axis. Significant correlation of the odds ratios was observed (‡, $P < 0.005$), even for the SNPs that showed moderate associations with rheumatoid arthritis (meta-analysis $P < 0.4$ in each population).

the two ancestry groups[17]. When the rheumatoid arthritis cases of the Japanese GWAS meta-analysis were stratified into anti-CCP–positive or rheumatoid factor–positive cases ($n = 3,209$) and controls ($n = 16,891$), similar results were observed (data not shown). Nevertheless, most of the SNPs assessed here are not necessarily causal variants, and further fine mapping of the loci is warranted to precisely evaluate the shared genetic predisposition between the populations.

Next, we compared regional associations within each of the loci and identified unique patterns in the *ARID5B* locus at 10q21 (**Supplementary Fig. 3**). In Japanese, three peaks of association were observed ($P = 1.0 \times 10^{-8}$ at rs10821944, $P = 5.7 \times 10^{-8}$ at rs10740069 and $P = 8.5 \times 10^{-6}$ at rs224311). These three variants were in weak linkage disequilibrium (LD) in Japanese ($r^2 < 0.10$), indicating independent associations with each of the other SNPs that satisfied a region-wide significance threshold of $P < 3.5 \times 10^{-5}$ (conditional $P = 4.3 \times 10^{-6}$, 1.7×10^{-5} and 1.8×10^{-5}, respectively) (**Supplementary Fig. 3**). In contrast, there was only one peak of association in Europeans ($P = 1.2 \times 10^{-6}$ at rs12764378; $r^2 = 0.59$ with rs10821944 in Europeans), and no additional association was observed in conditional analysis with rs12764378 (the smallest conditional $P = 2.2 \times 10^{-4}$), suggesting that the number of independent associations may be different at this locus in the two populations.

Finally, we conducted polygenic assessment for common variants showing modest associations to rheumatoid arthritis (those not meeting the genome-wide association threshold). This approach has been recognized to be a means to explain a substantial proportion of genetic risk[23]. For the SNPs that were shared between the two meta-analyses but not included in the validated rheumatoid arthritis susceptibility loci, we adopted LD pruning of the SNPs ($r^2 < 0.3$). We then evaluated the correlation of odds ratios of the SNPs between the two meta-analyses and observed a significant positive correlation ($r = 0.023, P < 1.0 \times 10^{-300}$). When the SNPs were stratified according to the *P* values in each meta-analysis, significant positive correlations of odds ratios were observed for the SNPs, even for those showing modest association ($P < 0.4$ in the meta-analysis of Japanese or Europeans; $r = 0.014–0.36$ for each *P* value range, $P < 0.005$ for each correlation test) (**Fig. 3c**). Correlations (r) of odds ratios observed herein suggest substantial overlap of the genetic risk of rheumatoid arthritis between the two populations, not only in the validated rheumatoid arthritis susceptibility loci but also at the loci showing nonsignificant associations. This suggests the usefulness of a meta-analysis approach involving multiple ancestry groups in identifying additional susceptibility loci.

In summary, we identified multiple new loci associated with rheumatoid arthritis through a large-scale meta-analysis of GWAS in Japanese. Multi-ancestry comparative analysis provided evidence of significant overlap in the genetic risks of rheumatoid arthritis between Japanese and Europeans. Thus, findings from the present study should contribute to the further understanding of the etiology of rheumatoid arthritis.

URLs. GARNET consortium, http://www.twmu.ac.jp/IOR/garnet/home.html; The BioBank Japan Project (in Japanese), http://biobankjp.org/; International HapMap Project, http://www.hapmap.org/; PLINK, http://pngu.mgh.harvard.edu/~purcell/plink/; EIGENSTRAT, http://genepath.med.harvard.edu/~reich/Software.htm; MACH and mach2dat, http://www.sph.umich.edu/csg/abecasis/MACH/index.

html; R statistical software, http://cran.r-project.org/; SNAP, http://www.broadinstitute.org/mpg/snap/index.php; NCBI GEO database, http://www.ncbi.nlm.nih.gov/geo/.

METHODS

Methods and any associated references are available in the online version of the paper at http://www.nature.com/naturegenetics/.

Note: Supplementary information is available on the Nature Genetics website.

ACKNOWLEDGMENTS

The authors acknowledge the essential role of the GARNET consortium in developing the study. In this study, the following GARNET members are included: CGM of RIKEN, University of Tokyo, the BioBank Japan Project, Kyoto University and IORRA. We would like to thank all the doctors and staff who participated in sample collection for the RIKEN cohort and the BioBank Japan Project. We thank K. Kobayashi and M. Kitazato for their technical assistance. We thank T. Raj for calculation of composite of multiple signals (CMS). We thank M. Kokubo for DNA extraction, GWAS genotyping and secretarial assistance. We would also like to thank H. Yoshifuji, N. Yukawa, D. Kawabata, T. Nojima, T. Usui and T. Fujii for collecting DNA samples. We thank Y. Katagiri for her technical efforts. We also appreciate the contribution of E. Inoue and other members of the Institute of Rheumatology, Tokyo Women's Medical University, for their efforts on the IORRA cohort. This study was supported in part by grants-in-aid from the Ministry of Education, Culture, Sports, Science and Technology (MEXT) in Japan, the Ministry of Health, Labour and Welfare (MHLW) in Japan, the Japan Society for the Promotion of Science (JSPS), Core Research for Evolutional Science and Technology (CREST), Solution-Oriented Research for Science and Technology (SORST), INSERM and the Okawa Foundation for Information and Telecommunications.

AUTHOR CONTRIBUTIONS

Y. Okada, C.T., K.I., Y. Kochi and K.O. designed the study and drafted the manuscript. Y. Okada, C.T., K.I., T.K., H.O., N.N., M.T., M.L., K. Tokunaga and M.K. managed genotyping and manipulation of GWAS data. Y. Okada, Y. Kochi, C.T. and K.I. managed genotyping of replication cohorts. Y. Okada, T.K., H.O., E.A.S., A. Takahashi and R.Y. performed statistical analysis. Y. Kochi, A.S., K. Myouzen, T. Sawada, Y. Nishoka, M.Y., T. Matsubara, S.W., R.T. and S.T. collected samples and managed phenotype data for the rheumatoid arthritis cohorts from the BioBank Japan Project and CGM, RIKEN. C.T., K.O., T.K., M.T., K. Takasugi, K.S., A.M., S.H., K. Matsuo, H. Tanaka, K. Tajima and M.L. collected samples and managed phenotype data for the rheumatoid arthritis cohorts from Kyoto University. K.I., T. Suzuki, T.I., Y. Kawamura, H. Tanii, Y. Okazaki and T. Sakaki collected samples and managed phenotype data for the rheumatoid arthritis cohorts from IORRA. Y. Kochi managed the data for the SLE and Graves' disease cohorts. A.S., C.T. and K.I. analyzed the sera of subjects with rheumatoid arthritis. E.A.S., F.A.S.K., P.K.G., J.W., K.A.S., L.P. and R.M.P. managed the data for the rheumatoid arthritis cohorts in European populations. A. Taniguchi, A. Takahashi, K. Tokunaga, M.K., Y. Nakamura, N.K., T. Minori, R.M.P., H.Y., S.M., R.Y., F.M. and K.Y. supervised the overall study.

COMPETING FINANCIAL INTERESTS

The authors declare no competing financial interests.

Published online at http://www.nature.com/naturegenetics/.
Reprints and permissions information is available online at http://www.nature.com/reprints/index.html.

1. Suzuki, A. *et al.* Functional haplotypes of *PADI4*, encoding citrullinating enzyme peptidylarginine deiminase 4, are associated with rheumatoid arthritis. *Nat. Genet.* **34**, 395–402 (2003).
2. Kochi, Y. *et al.* A functional variant in *FCRL3*, encoding Fc receptor–like 3, is associated with rheumatoid arthritis and several autoimmunities. *Nat. Genet.* **37**, 478–485 (2005).
3. The Wellcome Trust Case Control Consortium. Genome-wide association study of 14,000 cases of seven common diseases and 3,000 shared controls. *Nature* **447**, 661–678 (2007).
4. Remmers, E.F. *et al. STAT4* and the risk of rheumatoid arthritis and systemic lupus erythematosus. *N. Engl. J. Med.* **357**, 977–986 (2007).
5. Plenge, R.M. *et al. TRAF1–C5* as a risk locus for rheumatoid arthritis—a genomewide study. *N. Engl. J. Med.* **357**, 1199–1209 (2007).
6. Plenge, R.M. *et al.* Two independent alleles at 6q23 associated with risk of rheumatoid arthritis. *Nat. Genet.* **39**, 1477–1482 (2007).
7. Barton, A. *et al.* Rheumatoid arthritis susceptibility loci at chromosomes 10p15, 12q13 and 22q13. *Nat. Genet.* **40**, 1156–1159 (2008).
8. Suzuki, A. *et al.* Functional SNPs in *CD244* increase the risk of rheumatoid arthritis in a Japanese population. *Nat. Genet.* **40**, 1224–1229 (2008).
9. Gregersen, P.K. *et al. REL*, encoding a member of the NF-κB family of transcription factors, is a newly defined risk locus for rheumatoid arthritis. *Nat. Genet.* **41**, 820–823 (2009).
10. Kochi, Y. *et al.* A regulatory variant in *CCR6* is associated with rheumatoid arthritis susceptibility. *Nat. Genet.* **42**, 515–519 (2010).
11. Freudenberg, J. *et al.* Genome-wide association study of rheumatoid arthritis in Koreans: population-specific loci as well as overlap with European susceptibility loci. *Arthritis Rheum.* **63**, 884–893 (2011).
12. Terao, C. *et al.* The human *AIRE* gene at chromosome 21q22 is a genetic determinant for the predisposition to rheumatoid arthritis in Japanese population. *Hum. Mol. Genet.* **20**, 2680–2685 (2011).
13. Raychaudhuri, S. *et al.* Common variants at *CD40* and other loci confer risk of rheumatoid arthritis. *Nat. Genet.* **40**, 1216–1223 (2008).
14. Raychaudhuri, S. *et al.* Genetic variants at *CD28*, *PRDM1* and *CD2/CD58* are associated with rheumatoid arthritis risk. *Nat. Genet.* **41**, 1313–1318 (2009).
15. Stahl, E.A. *et al.* Genome-wide association study meta-analysis identifies seven new rheumatoid arthritis risk loci. *Nat. Genet.* **42**, 508–514 (2010).
16. Zhernakova, A. *et al.* Meta-analysis of genome-wide association studies in celiac disease and rheumatoid arthritis identifies fourteen non-HLA shared loci. *PLoS Genet.* **7**, e1002004 (2011).
17. Kurreeman, F. *et al.* Genetic basis of autoantibody positive and negative rheumatoid arthritis risk in a multi-ethnic cohort derived from electronic health records. *Am. J. Hum. Genet.* **88**, 57–69 (2011).
18. Nakamura, Y. The BioBank Japan Project. *Clin. Adv. Hematol. Oncol.* **5**, 696–697 (2007).
19. Yamanaka, H. *et al.* Influence of methotrexate dose on its efficacy and safety in rheumatoid arthritis patients: evidence based on the variety of prescribing approaches among practicing Japanese rheumatologists in a single institute-based large observational cohort (IORRA). *Mod. Rheumatol.* **17**, 98–105 (2007).
20. Yamada, R. *et al.* Association between a single-nucleotide polymorphism in the promoter of the human interleukin-3 gene and rheumatoid arthritis in Japanese patients, and maximum-likelihood estimation of combinatorial effect that two genetic loci have on susceptibility to the disease. *Am. J. Hum. Genet.* **68**, 674–685 (2001).
21. Tokuhiro, S. *et al.* An intronic SNP in a RUNX1 binding site of *SLC22A4*, encoding an organic cation transporter, is associated with rheumatoid arthritis. *Nat. Genet.* **35**, 341–348 (2003).
22. Okada, Y. *et al.* A genome-wide association study identified *AFF1* as a susceptibility locus for systemic lupus eyrthematosus in Japanese. *PLoS Genet.* **8**, e1002455 (2012).
23. Stranger, B.E., Stahl, E.A. & Raj, T. Progress and promise of genome-wide association studies for human complex trait genetics. *Genetics* **187**, 367–383 (2011).
24. Shimane, K. *et al.* A single nucleotide polymorphism in the *IRF5* promoter region is associated with susceptibility to rheumatoid arthritis in the Japanese patients. *Ann. Rheum. Dis.* **68**, 377–383 (2009).

[1]Laboratory for Autoimmune Diseases, Center for Genomic Medicine (CGM), RIKEN, Yokohama, Japan. [2]Department of Allergy and Rheumatology, Graduate School of Medicine, University of Tokyo, Tokyo, Japan. [3]Laboratory for Statistical Analysis, CGM, RIKEN, Yokohama, Japan. [4]Center for Genomic Medicine, Kyoto University Graduate School of Medicine, Kyoto, Japan. [5]Department of Rheumatology and Clinical Immunology, Graduate School of Medicine, Kyoto University, Kyoto, Japan. [6]Institute of Rheumatology, Tokyo Women's Medical University, Tokyo, Japan. [7]Division of Rheumatology, Immunology and Allergy, Brigham and Women's Hospital, Harvard Medical School, Boston, Massachusetts, USA. [8]Broad Institute, Cambridge, Massachusetts, USA. [9]Department of Rheumatology, Leiden University Medical Center, Leiden, The Netherlands. [10]Department of Human Genetics, Graduate School of Medicine, University of Tokyo, Tokyo, Japan. [11]Department of Rheumatology, Tokyo Medical University Hospital, Tokyo, Japan. [12]Yamanashi Prefectural Central Hospital, Yamanashi, Japan. [13]Department of Orthopaedic Surgery, Yukioka Hospital, Osaka, Japan. [14]Matsubara Mayflower Hospital, Hyogo, Japan. [15]Osaka Minami National Hospital, Osaka, Japan. [16]Department of Orthopedic Surgery, Tottori University, Tottori, Japan. [17]Department of Rheumatology, National Hospital Organization, Sagamihara Hospital, Kanagawa, Japan. [18]Center for Rheumatic Diseases, Dohgo Spa Hospital, Ehime, Japan. [19]Department of Rheumatology, Niigata Rheumatic Center, Niigata, Japan. [20]Saiseikai Takaoka Hospital, Toyama, Japan. [21]Division of Epidemiology and Prevention, Aichi Cancer Center Research Institute, Aichi, Japan. [22]Aichi Cancer Center Hospital and Research Institute, Aichi, Japan. [23]Department of Orthopaedic Surgery, Keio University, Tokyo, Japan. [24]Yokohama Clinic, Warakukai Medical Corporation, Yokohama, Japan. [25]Department of Psychiatry, Mie University School of Medicine, Mie, Japan. [26]Metropolitan Matsuzawa Hospital, Tokyo, Japan. [27]Graduate School of Education, University of Tokyo, Tokyo, Japan. [28]The Feinstein Institute for Medical Research, North Shore–Long Island Jewish Health System, Manhasset, New York, USA. [29]Rheumatology Unit,

Department of Medicine in Solna, Karolinska Institutet and Karolinska University Hospital, Stockholm, Sweden. [30]Arthritis Research Campaign–Epidemiology Unit, The University of Manchester, Manchester Academic Health Science Centre, Manchester, UK. [31]Division of Medicine, University of Toronto, Mount Sinai Hospital and University Health Network, Toronto, Ontario, Canada. [32]Commisariat a l'Energie Atomique (CEA), Institut Genomique, Centre National de Genotypage, Evry, France. [33]Fondation Jean Dausset, Centre d'Etude du Polymorphisme Humain, Paris, France. [34]Laboratory for Genotyping Development, CGM, RIKEN, Yokohama, Japan. [35]Laboratory of Molecular Medicine, Human Genome Center, Institute of Medical Science, University of Tokyo, Tokyo, Japan. [36]Laboratory for International Alliance, CGM, RIKEN, Yokohama, Japan. [37]Unit of Statistical Genetics, Center for Genomic Medicine Graduate School of Medicine Kyoto University, Kyoto, Japan. [38]Core Research for Evolutional Science and Technology (CREST) Program, Japan Science and Technology Agency, Kawaguchi, Japan. [39]Institut National de la Santé et de la Recherche Médicale (INSERM), Unité U852, Kyoto University Graduate School of Medicine, Kyoto, Japan. [40]These authors contributed equally to this work. [41]These authors jointly directed this work. Correspondence should be addressed to Y.K. (ykochi@src.riken.jp) or K.O. (ohmurako@kuhp.kyoto-u.ac.jp).